Nonaqueous potassium-ion full-cells: Mapping the progress and identifying missing puzzle pieces

Badre Larhrib, Louiza Larbi, Lénaïc Madec

Journal of Energy Chemistry 93 (2024) 384–399

Contents lists available at ScienceDirect

Journal of Energy Chemistry

journal homepage: www.elsevier.com/locate/jechem

http://www.journals.elsevier.com/journal-of-energy-chemistry/

Review

Nonaqueous potassium-ion full-cells: Mapping the progress and identifying missing puzzle pieces

Badre Larhrib [a,*], Louiza Larbi [b,c], Lénaïc Madec [a,d,e]

[a] Universite de Pau et des Pays de l'Adour, E2S UPPA, CNRS, IPREM, Pau, France
[b] Université de Haute-Alsace, Institut de Science des Matériaux de Mulhouse (IS2M), CNRS UMR 7361, F-68100 Mulhouse, France
[c] Université de Strasbourg, F-67081 Strasbourg, France
[d] Réseau sur le Stockage Electrochimique de l'Energie, CNRS FR3459, Amiens, France
[e] Institut des Matériaux Jean Rouxel (IMN), CNRS UMR 6502, Univ. Nantes, 44322 Cedex 3 Nantes, France

ARTICLE INFO

Article history:
Received 19 October 2023
Revised 10 January 2024
Accepted 10 January 2024
Available online 24 January 2024

Keywords:
K-ion full-cells
Potassium-ion batteries
Cross-talk
Solid-state batteries
Potassium reactivity
Electrolyte design
Electrode design

ABSTRACT

This review addresses the growing interest for potassium-ion full-cells (KIFCs) in view of the transition from potassium-ion half-cells (KIHCs) toward commercial K-ion batteries (KIBs). It focuses on the key parameters of KIFCs such as the electrode/electrolyte interfaces challenge, major barriers, and recent advancements in KIFCs. The strategies for enhancing KIFC performance, including interfaces control, electrolyte optimization, electrodes capacity ratio, electrode material screening and electrode design, are discussed. The review highlights the need to evaluate KIBs in full-cell configurations as half-cell results are strongly impacted by the K metal reactivity. It also emphasizes the importance of understanding solid electrolyte interphase (SEI) formation in KIFCs and explores promising nonaqueous as well as quasi- and all-solid-state electrolytes options. This review thus paves the way for practical, cost-effective, and scalable KIBs as energy storage systems by offering insights and guidance for future research.

Dr.Badre Larhrib was born in Marrakech (Morocco) in 1995. He obtained his Ph.D. degree in material chemistry and physics from the "Université de Pau et des Pays de l'Adour" (IPREM-CNRS), France, collaborating with various CNRS Laboratories (ICGM, ICMCB, and IS2M) in 2023. His doctoral research primarily revolved around electrode design, full-cell optimization, and interface investigations via XPS toward high performance potassium-ion batteries. Throughout his academic occupation, he delved into synthesizing layered oxides and phosphate materials for Li-ion and Na-ion batteries, alongside designing electrolytes for high-voltage Li-ion batteries. Presently, he serves as an R&D researcher at Tiamat Energy, directing his efforts toward the development of sodium-ion batteries.

Dr. Louiza LARBI received her Ph.D. degree in 2023 in material chemistry from the University of Haute Alsace (IS2M-CNRS) with a co-direction from the University of Montpellier (ICGM-CNRS), France. During her Ph.D, She was supervised by Dr. Camelia GHIMBEU and Dr. Laure MONCONDUIT, her work was focused on the development of carbon anodes for the new generation of potassium-ion batteries.She iscurrently a post doctoral researcher at Sorbonne University (LCMCP-CNRS) working on the development of hybrid solid electrolyte for all-solid-state-batteries.

* Corresponding author.
E-mail addresses: badre.larhrib@tiamat-energy.com, badre.larhrib@univ-pau.fr (B. Larhrib).

https://doi.org/10.1016/j.jechem.2024.01.033

Dr.Lénaïc Madec was born in Mayenne (France) in 1986. After a master in chemistry of materials in Paris, he obtained a Ph.D in electrochemistry (2012) at the University of Nantes then continued as a postodctoral fellow on redox flow battery. In 2013, he joined the University of Halifax, Canada, as a postdoctoral fellow with Prof. J. Dahn to study aging of Li-ion cells through XPS analysis. In 2015, he pursued XPS analysis on Li-ion anodes as a postoctoral fellow in the French RS2E network (IGCM-IPREM labs). In 2016, he obtained a CNRS researcher position at the Institute of Analytical Sciences and Physico-Chemistry for Environment and Materials, Pau, where he developed researches on K-ion and solid-state batteries as well as supercapacitors with a focus on electrochemical/aging mechanisms through surface analysis (XPS, Auger) combined with cross-section samples preparation. Recently, he proposed *operando* methods for XPS / SEM-Auger analysis to study Li plating and interphase formation in solid-state batteries. Since 2023, he joined the Institut des Matériaux Jean Rouxel, Nantes to pursue his work as a CNRS researcher.

1. Introduction

Potassium-ion batteries are being explored as a potential alternative to lithium-ion batteries (LIBs) and sodium-ion batteries (NIBs) for large-scale renewable energy storage systems. These systems require affordable and abundant precursors and materials. In that direction, potassium (K), which is highly abundant (2.1 wt.% of the Earth's crust), can be used with graphite as negative active material and aluminium as current collector [1–3]. KIBs are also expected to have high power performance due to the low desolvation energy of K^+ (~119 kJ mol^{-1}) vs. Na^+ (~158 kJ mol^{-1}) and Li^+ (~216 kJ mol^{-1}) in propylene carbonate based-electrolytes as well as the small solvated shell radius of K^+ (~3.6 Å) vs. Na^+ (~4.6 Å) and Li^+ (~4.8 Å) in the same electrolyte [1,4]. However, there are still some challenges to overcome: the high atomic mass of potassium (39.1 g mol^{-1}) and the larger Shannon's ionic radius of K^+ (1.38 Å) compared to Na^+ (1.02 Å) and Li^+ (0.76 Å), as well as potential safety issues such as potassium plating [5–7]. Moreover, K-ion half-cells are strongly dependant of the K metal electrode (i.e. plating/stripping, coulombic efficiency, polarization, aging, cross-electrodes contamination due to the K metal reactivity with electrolytes) and thus cannot provide a complete performance assessment. Thus it appears mandatory to evaluate KIBs performance and perform solid electrolyte interphase studies in K-ion full-cells. Finally, mastering the procedure for transitioning from KIHCs to KIFCs becomes of high importance considering these factors. Overall, critical parameters, boosting strategies and progress map of potassium-ion full-cells are currently lacking in the KIBs literature.

This review thus summarizes the state-of-art of KIFCs. Indeed, an examination of the papers published between 2012 and the end of 2023 (Fig. 1) reveals that researchers have displayed increasing interest and focus on the development of K-ion full-cells in parallel to the research on K-ion half-cells toward the practical use of K-ion batteries. To the best of our knowledge, this is the first comprehensive report that reviews nonaqueous. To this end, this review first focuses on key parameters that govern half-cells, i.e. the role and impact of K metal to show why full-cells should be preferred regarding both electrochemical and interfaces properties difference. Comparing these two cell configurations is crucial for gaining a comprehensive understanding of KIFCs. Moreover, interface properties play a significant role in KIFCs, and studying their features is essential for addressing key challenges. Second, a map of the latest achievements in KIFCs is presented. Especially for nonaqueous electrolytes, which have shown promising results in terms of improved performance and stability. Additionally, the exploration of quasi- and all-solid-state electrolytes based-K-ion full-cells is also discussed as it has provided alternative pathways for advancing K-ion technology. Third, various improvement strategies are discussed to further enhance KIFCs performance, including the optimization of electrolytes to achieve stable passivation layers, screening of electrodes materials for power and energy applications and a guideline (i.e., optimization of balancing ratio, diameter ratio, and electrolyte amount) toward optimized KIFC parameters for reliable cells. These strategies, along with other innovative approaches, aim to drive the development of efficient and reliable KIFCs. Thus, the integration of these aforementioned parameters should lead to a novel phase in the development of KIBs as energy storage systems that are practical, affordable, and scalable.

2. Why going from half- to full-cells?

Understanding the SEI growth, aging, and degradation mechanisms is essential to ensure the KIBs development and to obtain reliable studies, particularly in regards to the high reactivity of the potassium metal. To achieve this target, we will thoroughly investigate the difference between half- and full-cells from the electrochemical point of view then the interfaces one.

2.1. Electrochemical difference and issues

The practical application of half-cells using potassium metal as an anode in K-ion batteries is hindered by K metal passivation, high polarization, ageing and possible dendritic growth, which can lead to potential safety hazards caused by the high reactivity and low melting point of potassium metal [8]. In particular, the plating

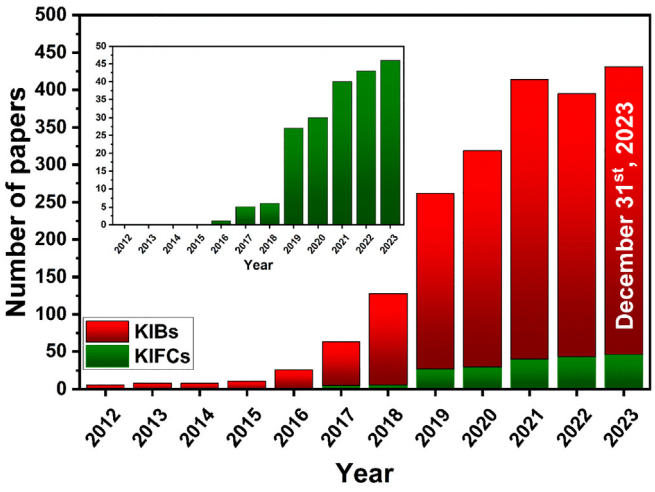

Fig. 1. Number of articles related to KIBs and specifically to KIFCs published from 2012 to December 31st, 2023 (obtained from Web of Science).

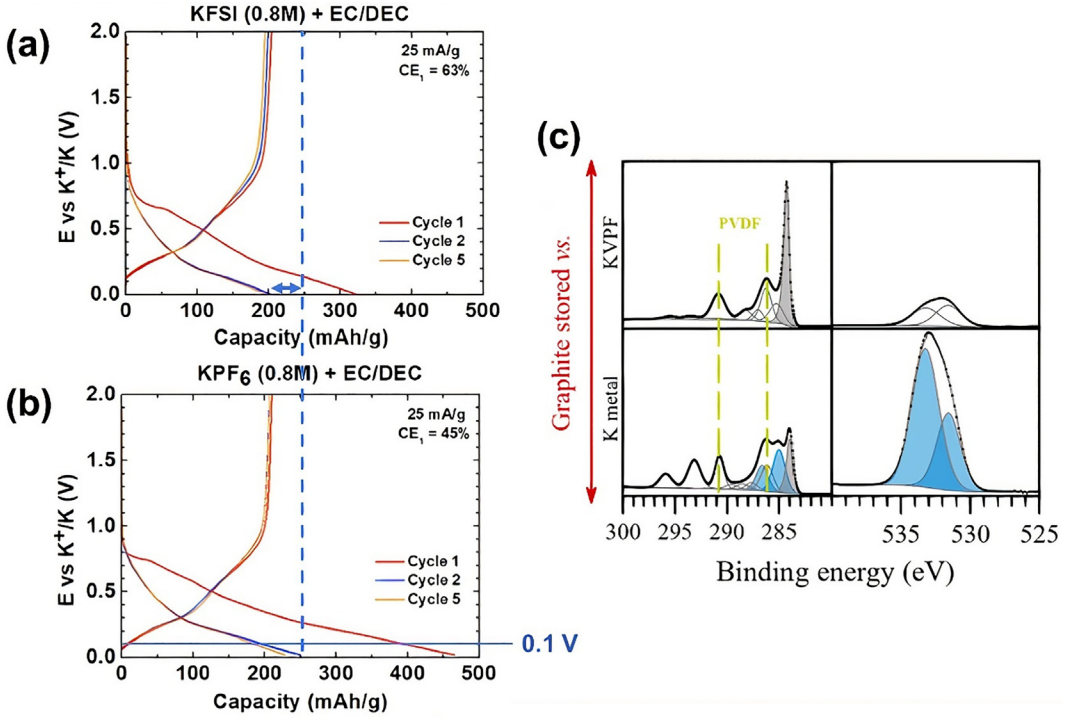

Fig. 2. Electrochemical performance of carbon nanofibers (CNF) vs. K. Galvanostatic charge/discharge at 25 mA g^{-1}. (a) 0.8 M KPF_6 and (b) KFSI in EC:DEC. Reproduced with permission from Ref. [11]. Copyright 2020, Elsevier. (c) Comparison of K 2*p*−C 1*s* and O 1*s* X-ray photoelectron spectroscopy (XPS) core-level spectra of graphite electrodes following 24 h of storage with either a $KVPO_4F$ or potassium metal electrode, utilizing a 0.8 M KPF_6 in EC:DEC electrolyte: normalized intensities for comparative analysis. Highlighted in blue are peaks indicating electrolyte degradation products. Reproduced with permission from Ref. [8]. Copyright 2022, American Chemical Society.

and stripping process of K metal exhibits a relatively low coulombic efficiency (CE) of less than 70% and high polarization, even at low rates, when using KPF_6 (hexafluorophosphate)-based carbonate electrolytes [9]. This thus significantly impact the rate performance and capacity retention evaluation in half-cells [10]. Substituting KFSI (i.e., potassium bis(fluorosulfonyl)imide) in carbonate electrolytes generally increases polarization by at least 0.1 V (Fig. 2a and b) [11].

This is due to the improved passivation of K metal through the formation of a more inorganic solid electrolyte interphase based on degradation products of the FSI^- anion [8]. Interestingly, in half-cells, it is better to use highly concentrated KFSI DME (dimethoxyethane) electrolytes as a substitute from carbonate electrolytes as these electrolytes offer the highest K plating/stripping CE, over 95% [9] and exhibit stable polarization across low, moderate, and high current densities [12]. Moreover, in half-cells, the aging of K metal, which involves passivation and impedance increase during cycling, also alters the performance evaluation [13] but is almost always neglected so far in the existing literature. Moreover, in half-cells, the irreversible consumption of active potassium derived from SEI formation at the cathode is overcompensated by the unlimited source of K at the anode while in full-cells; this phenomenon becomes evident and will negatively impact the cell-lifetime due to the limited K content. In contrast, in full-cells, the irreversible consumption of active K will significantly impact the capacity loss and thus the overall performance, which can then be minimized using electrolyte optimization for instance.

2.2. Interfaces properties, difference, and issues

Because almost all electrochemical reaction sites are located at the different interfaces throughout KIBs cells, the feature of these interfaces is important. Fig. 3 depicts the different interfaces for half- and full-cells and their main properties for typical nonaqueous liquid electrolyte.

2.2.1. Electrode/Electrolyte interface

During electrochemical cycling, different side reactions can occur at the electrode particles surface that consume electrons and M^+ (M^+: metal, K^+ in our case) cations. These reactions can cause the electrolyte degradation (salt and/or solvent), which is evident from the electrochemical curves that generally show significant irreversible capacity upon the first few cycles. As a result, electrolyte degradation products lead to the formation of passivation layers at the electrode particles surface called SEI for the negative electrodes, and cathode electrolyte interphase (CEI) or solid permeable interface (SPI) for the positive electrodes [14,15]. For clarity, note that despite that these interphases are all SEI, the naming difference for negative and positive electrodes originates from the different properties of these passivation layers as observed and proposed in Li-ion literature.

In half-cells, Caracciolo et al. [8] elucidated the complete electrolyte degradation pathways at the K surface of the commonly used 0.8 M KPF_6 or KFSI EC:DEC (Ethylene Carbonate:Diethyl Carbonate) electrolytes by combining X-ray photoelectron spectroscopy (solid products analysis) with gas chromatography (GC)-mass spectrometry and GC/Fourier transform infrared spectroscopy (gas product analysis). Note first that by comparison with Li metal in $LiPF_6$ EC:DEC, they pointed out an higher electrolyte reactivity at the K metal surface compared to the Li metal surface due to the salt cation effect. Indeed, without salt, the K and Li metal showed the same EC:DEC reactivity while with the addition of MPF_6 salt (M = Li or K), the SEI was mostly based on LiF from the PF_6^- degradation and on solvent degradation products for Li and K, respectively. It is worth noting that this recent experimental study is in perfect agreement with theoretical calculations showing that for the Li^+-solvent complex is much more stable than the

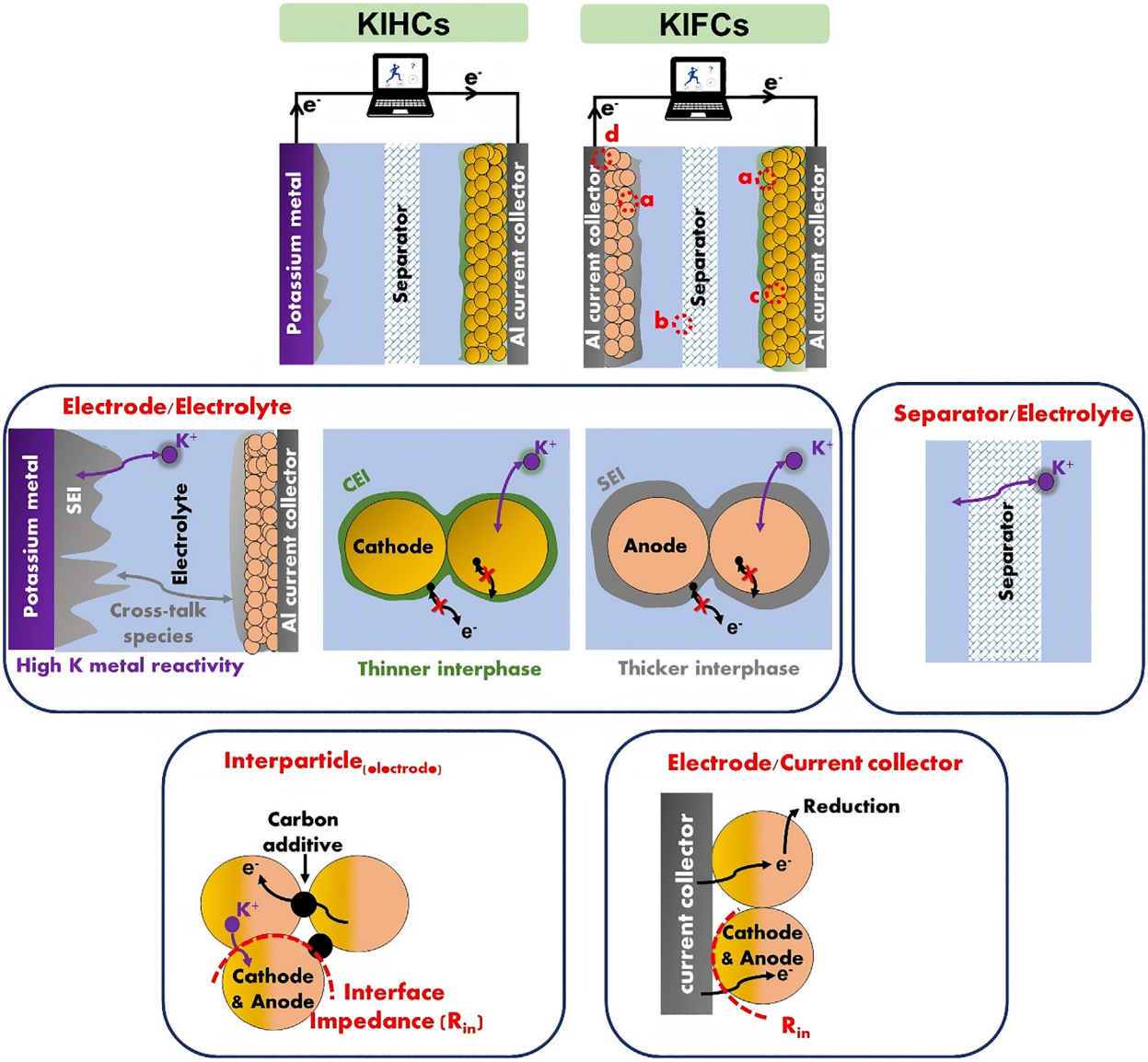

Fig. 3. Schematic illustration of half- and full-cells and their respective interfaces features.

K^+-solvent complex for MPF_6 (M = Li or K) in carbonates [16,17]. More importantly, the study by Caracciolo et al. [8] also pointed out an anion effect as the K surface, the SEI was mostly organic with KFF_6 (from the solvent degradation) while it was mostly inorganic (from the FSI^- degradation) with KFSI, in agreement with theoretical calculation showing that in the K^+-solvent-anion complex (with carbonates), the FSI^- is much closer to K^+ than PF_6^-, which stabilize the solvent reduction [16,17].

Another important consideration for half-cells, is the reactivity of the electrolyte at the K surface that forms electrolyte degradation products (i.e., KF, K_2CO_3, ROK) [8], which migrate to the working electrode, i.e. causing cross-talk between electrodes, and more importantly regardless of the electrolyte or electrode used and even at open circuit voltage (i.e., graphite electrode) [8,18,19] (Fig. 2c). At this point it very is important to note that most of the anode SEI analyzed in K-ion half-cells using KPF_6 and KFSI EC:DEC electrolytes [19–21] showed similar composition to the K metal SEI analyzed by Caracciolo et al. [8] so that considering the cross-talk phenomenon, it is impossible to assess that the anode SEI is formed only at its surface and does not originate mostly from the K metal side.

As an alternative, the use of potassium metal is possible in the case of quasi- and all-solid-state electrolytes for which the interface between the electrode and electrolyte may lead to nearly no irreversible consumption of active K as long as an appropriate electrochemical window is maintained, which depends on the specific electrolyte used [22]. However, the large interface impedance (R_{in}) and incompatibility resulting from the solid electrode/solid electrolyte contact significantly hinder the movement of K ions, which results in a low cycle stability and limited rate capability. In other words, while the electrode/electrolyte interface is more stable with quasi- and all-solid-state electrolytes compared to liquid electrolytes, the poor compatibility and large interface impedance do present significant challenges to the efficient operation of these devices.

2.2.2. Separator/electrolyte interface

Glass fiber (GF) is the most widely used separator among the reported studies on KIBs, due to its good wettability and ability to uptake a large amount of electrolyte. This is also due to the need of a glass fiber separator in contact with K metal in half-cells, which may be explained by a much better electrolyte wettability

of the K surface thanks to the GF separator affinity with the K metal compared to a PP/PE/PP trilayer separator (so-called Celgard) [23]. However, traditional Celgard membranes show poor compatibility and wettability with many electrolyte systems (such as PC and EC-PC), resulting in large impedance or battery failure [24,25]. Finally, the use of Celgard or Solupor separators that have low thicknesses of ~25 μm and high porosities (~53%, and ~78%, respectively) should be preferred for full-cells and in any case, their use is crucial to meet the needed specifications for full-cells assembly [26,27].

2.2.3. Inter-particles interface

In all systems, the interface between particles is critical for efficient ion migration and electron transfer. Various engineering strategies such as coating, composite, and morphology design (1D-3D) have been proposed to address this issue so far [2,28–30]. Furthermore, the electrode materials/carbon (i.e. conductive additive) interfaces should ensure a good electronic percolating network [31]. At this point, further studies are needed to develop KIFCs.

Finally, for quasi- and all-solid-state electrolyte, the electrolyte interparticle interface also requires a rapid transfer of K^+ ions while minimizing electronic transmission. Also, for such electrolytes, the interface with the electrodes materials often presents a challenge due to the large interface and/or grain boundary impedances. Overcoming this challenge will be one of the key to the development of solid-state batteries.

2.2.4. Electrode/current collector interface

The existence of this interface requires the binder to meet various requirements such as adhesion between the active material and conductive additive (carbon) particles together with the current collector surface and an electrochemical stability of this binder. If the adhesion is weak, the electrode may delaminate from the current collector or even separate completely, which can lead to battery failure. It have been demonstrated that an improvement on the electrode/current collector interface reduce the charge-transfer resistance, which is attributed to the removal of the native insulating oxide surface layer of the collector and to the enhanced adhesion at the active material/current collector interface [32]. Thus, in-depth interface studies are needed for further development of K-ion full-cells as this interface have been barely studied so far [33].

To conclude, KIFCs with anodes other than K metal (i.e., graphite [34], carbon composite [35], MXene [36], red phosphorus [37] and other designed materials [38–41]) are recommended to overcome the above-discussed K metal issues. In other words, half-cells with K metal present to many issues to deal with so that full-cells, i.e. KIFCs are mandatory to evaluate KIBs performance, SEI analysis and aging mechanisms. Likewise, full-cells, when compared to half-cells, provide more reliable performance evaluation of KIBs. Furthermore, interfaces within KIFCs, including the electrode/electrolyte, separator/electrolyte, inter-particles, and electrode/current collector interfaces, play a crucial role in KIFC performance and require comprehensive study for the industrialization of KIBs so that it is important to address challenges like SEI growth, interface impedance, and electrode material compatibility to achieve efficient and stable KIFCs. Overall, a detailed investigation of these interfaces is vital for advancing KIFCs.

3. Latest achievements on K-ion full-cells

Due to the intense study of KIBs, there is an increasing interest among researchers in KIFCs, which is expected to lead to their practical application. Literature statistics indicate that while KIFCs focus on a variety of research objects, such as electrode materials and electrolytes. On the other hand, for quasi- and all-solid-state based KIFCs, the first focus is on electrolytes development. This section will provide a summary of the recent progress made in researching various KIFCs and delve into the strategies employed to tackle the issues.

3.1. Nonaqueous liquid based-electrolytes

In 2017, several research groups presented their findings pioneer works on KIFCs. The group of S. Komaba [42] presented a PB//-graphite full-cell (PB stands for Prussian Blue, here $K_{1.75}Mn[Fe(CN)_6]_{0.93}$, i.e. K-MnHCFe) that delivered a reversible capacity of 110 mA h g^{-1} with a mean operating voltage of 3.5 V, as shown in Fig. 4(b_1). Note that the corresponding electrochemical behaviour of graphite//K and K-MnHCFe//K half-cells were also presented as references (Fig. 4a1). Also, Fig. 4(c_1) represents that the full-cell also demonstrated acceptable capacity retention of 75% over 60 cycles. Regarding the rate capability, the full-cell shows good rate performance even at a current density of 2000 mA g^{-1} (i.e. equivalent to 15 $C_{discharge\text{-}rate}$) with a capacity of 60 mA h g^{-1}, as shown in Fig. 4(d_1). However, the electrode loading was not specified in this study. Table S1 illustrates consistently low loading across the majority of the referenced papers. Wang et al. [43] presented a KIFC based on interconnected $K_{0.7}Fe_{0.5}Mn_{0.5}O_2$ nanowires and soft carbon, which achieved a high initial coulombic efficiency (ICE) of ~92% in the first cycle. Although the cell delivered a discharge capacity of 82 mA h g^{-1} at 40 mA g^{-1}, the capacity retention was ~90% after 50 cycles, and a low operating voltage of 2.0 V was observed. However, the cell showed considerable long-term cycling stability even when tested at 100 mA g^{-1}. In the same year, a $K_{0.6}CoO_2$//graphite full-cell was tested, which delivered a specific discharge capacity of ~53 mA h $g^{-1}_{cathode}$ at a rate of 3 mA g^{-1}, with a capacity retention of 50% over 5 cycles [44]. Note that in this work, the graphite anode was cycled between 0.01 and 1.5 V before the full-cell assembly due to the large irreversible capacity in the first discharge process so that the capacity retention of the full is more likely overestimated. Note also that no coin-cell assembling optimization was done. Moreover, a 3,4,9,10-perylene tetracarboxylicacid dianhydride (PTCDA)//pyridinic N-doped porous carbon monolith (PNCM) full-cell was assembled by pairing the as-obtained PNCM anode with PTCDA cathode [45]. The obtained KIFC exhibited discharge capacities of 245, 168, 143, 114, 99, and 85 mA h g^{-1} (calculated based on the mass of the PNCM anode) at increasing current densities of 50, 100, 200, 500, 1000, and 2000 mA g^{-1}, respectively. After 70 cycles, the full-cell delivered a capacity retention of 37% at 100 mA g^{-1}. However, the capacity fades at long term cycling is probably due to PTCDA dissolution in carbonate-based electrolytes, which limits its practical use.

In 2019, various KIFC systems were investigated for their capacity and long-term cycling performance. One system was the $K_3V_2(PO_4)_3/C//K_3V_2(PO_4)_3/C$ (KVP/C) symmetric full-cell, which exhibited an initial CE of 91.7% with charging and discharging capacities of 88 and 80.9 mA g^{-1} during the first cycle [46]. The cell maintained a reversible capacity of 88.6% over 500 cycles, with an average voltage of 2.3 V but with cathode and anode mass loadings of only 1 mg cm^{-2}. Another K-ion full-coin cell system was investigated in the same year, which developed reduced graphite (KC_8) as the anode and oxidized potassium 9,10-anthraquinone-2,6-disul fonate (KQ26DS) as the cathode [47]. This system delivered a capacity of 82 mA h g^{-1} at 50 mA g^{-1} with a capacity retention of 33% over 2500 cycles and an average voltage of 1.3 V. The KQ26DS//KC_8 system exhibited a rate performance of 46 mA h g^{-1} at 1000 mA g^{-1}. Another group investigated the performance of a PTCDA//KC_8, where the positive and negative electrodes were pre-cycled vs. K metal [48] to preform the SEI in half-cells and then limit the electrolyte degradation in the full-cell. This system exhib-

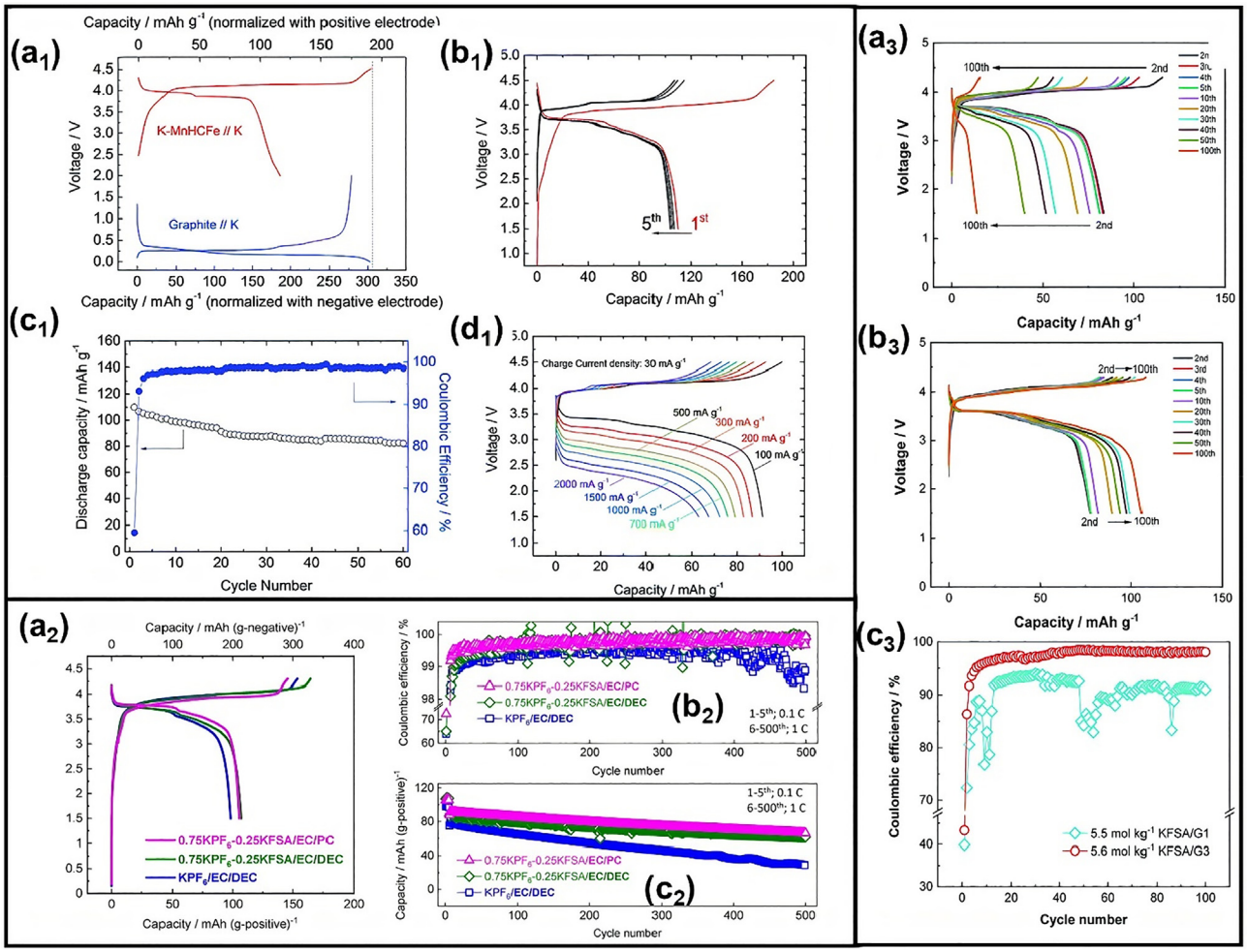

Fig. 4. (a_1) Initial charge-discharge profiles of K-MnHCFe//K and graphite//K in a half-cell configuration; (b_1) electrochemical cycling profiles of the K-ion cell, K-MnHCFe/graphite, cycled at a current rate of 30 mA $g^{-1}_{cathode}$ in a voltage range of 1.5–4.5 V; (c_1) long term cycling capacity and efficiency, and (d_1) rate performance of the K-ion full-cell, charge current density is 30 mA g^{-1} and discharge current densities are from 100 to 2000 mA g^{-1}. Reproduced permission from Ref. [42]. Copyright 2017, Royal Society of Chemistry. (a_2) Initial charge/discharge profiles of graphite//$K_2Mn[Fe(CN)_6]$ full-cell filled with 0.75 mol kg^{-1} KPF_6/EC/DEC, 1.0 mol kg^{-1} $K(PF_6)_{0.75}(FSA)_{0.25}$/EC/DEC, and 1.0 mol kg^{-1} $K(PF_6)_{0.75}(FSA)_{0.25}$/EC/PC, ($b_2$) evolution of their specific capacity, and (c_2) evolution of their CE. The current density was 15.5 mA $g^{-1}_{cathode}$ from 1st to 5th cycle and 155 mA $g^{-1}_{cathode}$ from 6th to 500th cycle. Reproduced with permission from Ref. [52]. Copyright 2020, American Chemical Society. (a_3) Charge-discharge profiles of graphite//$K_2Mn[Fe(CN)_6]$ full-cells filled with 5.5 mol kg^{-1} KFSI/G1 + 0.5 wt% vinylene carbonate (VC), and (b_3) 5.6 mol kg^{-1} KFSI/G3 + 0.5 wt% VC, (c_3) evolution of their CE upon 100 cycles. Reproduced with permission from Ref. [53]. Copyright 2020, Royal Society of Chemistry.

ited an average voltage of 1.9 V and delivered a capacity of 140 mA h g^{-1} at 50 mA g^{-1} with 73% of capacity maintained over 30 cycles. The rate performance for this system was similar to the KQ26DS//KC_8 system, exhibiting 46 mA h g^{-1} at 1000 mA g^{-1}. Still in 2019, another group proposed a KIFC system based on P2-$K_{0.75}MNFO_2$ and hard carbon as cathode and anode electrode materials, respectively [49]. The full-cell exhibited an initial discharge capacity of 60 mA h g^{-1} and stable long-term cycling, with approximately 60% capacity retention over 1000 cycles at 0.2 C and an average voltage of 2.1 V. The diffusion pathways of K ions and the activation barrier energy for K^+ diffusion in the P2-$K_{0.75}MNFO_2$ structure were calculated using the nudged elastic band method, supporting the experimental observation of the excellent power capability of the P2-$K_{0.75}MNFO_2$ active material. Another study used a P2-$K_{0.83}[Ni_{0.05}Mn_{0.95}]O_2$//hard carbon full-cell system, which demonstrated a high capacity of 135 mA h g^{-1} (2.1 V average voltage) and exceptional long-term cyclability, with a capacity retention of approximately 80% over 300 cycles [50]. However, the active material loading was only 3 and 2.3 mg cm^{-2} for cathode and anode materials, respectively. Ex situ XRD and TEM analysis of electrodes before and after extensive cycling confirmed the structural stability of the P2-$K_{0.83}[Ni_{0.05}Mn_{0.95}]O_2$. The post-cycled electrode maintained its high crystallinity, sharp features of (002) and (004) peaks for the P2 phase, and slight variation in lattice parameters. TEM analysis of electrodes before and after extensive cycling further confirmed that the post-cycled electrode maintained the original morphology of the pre-cycled electrode without morphological degradation after 500 cycles. However, this finding was reached after the cathode and anode were precycled vs. K metal so that electrolyte degradation was reduced in the full-cell, which more likely led to an overestimation of the long term capacity retention. Still in 2019, Komaba's group [51–53] conducted three studies on $K_2MnFe(CN)_6$//graphite full-cells. In the first study, the group investigated the impact of electrolytes on the cell's performance [51]. They found that using a 1 M K[FSA]/[C_3C_1pyrr][FSA] electrolyte resulted in a capacity retention of 76% after 200 cycles with an initial discharge capacity of 91 mA h g^{-1}. Between the 2nd and 200th cycles, the average voltage and CE were 3.2 V and 99.5%, respectively, which was better than anything previously reported for KIFCs. The use of FSA-based ionic liquid improved stability and passivation ability, preventing undesired side reactions at both the graphite anode and Prussian blue ana-

logue cathode interfaces. Note, however, that the active mass loading was still limited to 4.0 and 2.0 mg cm^{-2} for the cathode and anode, respectively. In the second study, the group evaluated the use of different KFSI-KPF_6-binary based electrolytes and selected polytetrafluoroethylene (PTFE) and carboxymethylcellulose (CMC) binders for the positive and negative electrodes, respectively [52]. They found that the KICF with 0.75KPF_6-0.25 M KFSI EC/PC electrolyte demonstrated the highest initial coulombic efficiency, ICE of 72.5% and the smallest polarization, delivering a reasonably high reversible capacity of 105 mA h g^{-1} with an average voltage of 3.6 V (Fig. 4a2 and b2). The capacity retentions of 0.75 M KPF_6-0.25 M KFSI EC:DEC and 0.75 M KPF_6-0.25 M KFSI EC:PC cells after 500 cycles were 72% and 75%, respectively. Such capacity retention were far superior to the full-cell using the commonly used 0.75 M KPF_6 EC:DEC based electrolyte (37%), as shown in Fig. 4(c_2). An increase in the average voltage was noticed from 3.2 to 3.6 V compared to the previously mentioned study with ionic liquid-based electrolyte. It is also significant that the full-cells maintained more than 85% of reversible capacity at a 5 C discharge rate compared to that of 0.1 C regardless of the electrolyte, which demonstrates good rate capability for the full-cells [52]. Note, however, that such high rate capacity were achieved for cathode and anode active material loading of 4.0 and 2.0 mg cm^{-2}, respectively. In the third study, the group investigated the electrochemical performance of KIFCs using two different glyme-based highly concentrated electrolyte solutions: 5.5 mol kg^{-1} KFSI G1 + 0.5 wt% vinylene carbonate (VC) and 5.6 mol kg^{-1} KFSI G3 + 0.5 wt% VC. The addition of 0.5 wt% VC into the electrolyte solution was effective in suppressing the initial irreversible capacity of the full-cells [53]. The G1 and G3 cells delivered reasonable initial discharge capacities of 86 and 79 mA h g^{-1}, respectively (Fig. 4a3 and b3). The cell with G1 showed a significant decrease in discharge capacity after 100 cycles, while the cell with G3 exhibited considerably higher cycle performance, maintaining high CE over 100 cycles (Fig. 4c3). The study suggests that KFSI G3 electrolytes are more suitable for high voltage (3.95 V) than KFSI G1 electrolytes. The high oxidation stability of KFSI G3 electrolytes was explained by the strong interaction of K ions with long glymes (Solution structures were investigated using Raman spectroscopy).

In 2021, an investigation was conducted on a natural graphite vs. Prussian blue/polyvinylpyrrolidone/reduced graphene oxide (PB/PVP-rGO) as full-cell [54]. The intercalated graphite (KC_8) was employed as the anode for the full-cell electrochemical testing, prepared through pre-potassiation vs. K metal. The rate performance of the composite-based full-cell was evaluated with a current density range of 0.5–10C. PB/PVP-rGO displayed excellent rate performance, achieving capacities of 127.9, 115.5, 104.7, 89.0, and 77.0 mA h g^{-1} at 0.5, 1, 2, 5, and 10 C, respectively. Furthermore, PB/PVP-rGO//KC_8 cells exhibited 88.1% of capacity retention over 150 cycles at 1C with an average voltage of 3.3 V.

In 2022, Li et al. [55] studied a new type of Pitch-derived soft carbon vs. $K_{1.69}Mn_{0.779}Ni_{0.221}[Fe(CN)]_{0.93}{\cdot}0.392H_2O$ as full-cell. The assembled full-cell also exhibited high-rate capability, maintaining a discharge capacity of 62.5 mA h g^{-1} at a current density of 500 mA g^{-1}. When the current density was brought back to 50 mA g^{-1}, a reversible capacity of 87.2 mA h g^{-1} was recovered. As well, the cycling performance was evaluated at 100 mA g^{-1}, and 89.6% of the initial capacity (71.8 mA h g^{-1}) was maintained after 100 cycles, with an average potential of 3.83 V.

In 2023, research was conducted on a $K_{0.95}Cs_{0.05}VPO_4F$//-graphite full-cell that used Cs^+ doping to lower the energy barrier for ion diffusion and volume change during the potassiation/depotassiation process of the cathode active material [56]. This resulted in an important improvement in the K^+ diffusion coefficient and provided stability to the positive electrode framework. The full-cell had a high average voltage of 3.93 V and provided a capacity of 103 mA h g^{-1} at 100 mA g^{-1}. The capacity retention was high, with 90% of the capacity being maintained over 1000 cycles. Additionally, the full-cell could reach a capacity of 62.7 mA h g^{-1} when cycled at 2000 mA g^{-1}. The Cs^+ doping approach used in this study could have a significant impact on the development of high-performance cathode material for KIBs.

In the field of KIFC, Table S1 provides a comprehensive summary of the full-cell system evaluated so far, highlighting its tremendous potential. However, upon thorough analysis, we notice that most studies involve a pre-cycling of the electrodes versus K-metal before assembling the full-cells, which first is not practical and second more likely leads to overestimation of the full-cells capacity retention. Also importantly, the practical cathode active mass loading should be higher than 8 mg cm^{-2} (ideally as high as possible) for an up-scaled application while it remains always between 0.5 and 6 mg cm^{-2} in all studies so far [57]. Additionally, many investigations still utilize glass fiber (GF) as a separator, which is not optimal for practical use.

3.2. Quasi- and all-solid-state based-electrolytes

Despite significant progress in the development of KIBs since 2015, there are still several challenges that need to be addressed, particularly the issue of severe side reactions between the electrolyte and K metal due to its high reactivity [8]. These reactions can result in an unstable SEI and low CE. Therefore, the selection of an excellent electrolyte is crucial for the advancement of KIBs. Unfortunately, there has been a lack of systematic research on electrolytes and their role in performance, taking into consideration safety concerns [58].

To overcome this limitation, quasi and all-solid-state electrolytes have gained attention, as they are non-flammable and do not present risks of leakage or explosion. These electrolytes can be categorized into inorganic, organic, and hybrid-based types [59]. While inorganic-based solid-state electrolytes (SSE) have been studied for their high ionic conductivity, their synthesis typically requires high temperatures and they tend to have poor interface contact with electrodes, hindering further improvement [58]. On the other hand, organic-based electrolytes offer simple preparation, excellent chemical stability, and good interface contact with electrodes, and have garnered significant interest [22,60]. However, their low ionic conductivity at room temperature limits their application, especially for low-operating temperatures. Therefore, hybrid based SSE could be a promising alternative that combines the features of all the mentioned types.

The quasi and all-solid-state electrolytes application in KIBs gained momentum in 2018 when the synthesis of inorganic 3D open-framework potassium ferrite, $K_2Fe_4O_7$, was successfully achieved through an hydrothermal process [61]. The framework of $K_2Fe_4O_7$ comprises FeO_6 octahedral and FeO_4 tetrahedral units, allowing for high ionic conductivity through the channels. The polycrystalline sample exhibited an ionic conductivity of 5×10^{-2}-S cm^{-1} at room temperature, with an activation energy of 0.08 eV (7.7 kJ mol^{-1}). Notably, the all-solid-state potassium metal battery with a Prussian blue cathode demonstrated exceptional rate capability, delivering a reversible specific capacity of 13 mA h g^{-1} at a high charge/discharge rate of 250 C (charge/discharge in 14 s), and a reversible specific capacity of 87 mA h g^{-1} for the cell cycled at 1 C (charge/discharge in 1 h). These results go well beyond those reported for KIBs using liquid electrolytes vs K metal. In the same year, Huifang Fei et al. [62] presented a study on all-solid-state electrolytes based on 3,4,9,10-perylene-tetracarboxylicacid-dianhydride (PTCDA) as the positive electrode and solid polymer electrolyte (SPE) for the first time. The SPE employed was poly(propylene carbonate)-KFSI with cellulose nonwoven backbone (PPCB-SPE), which exhibited an ionic conductivity of 1.36×10^{-5} S cm^{-1}

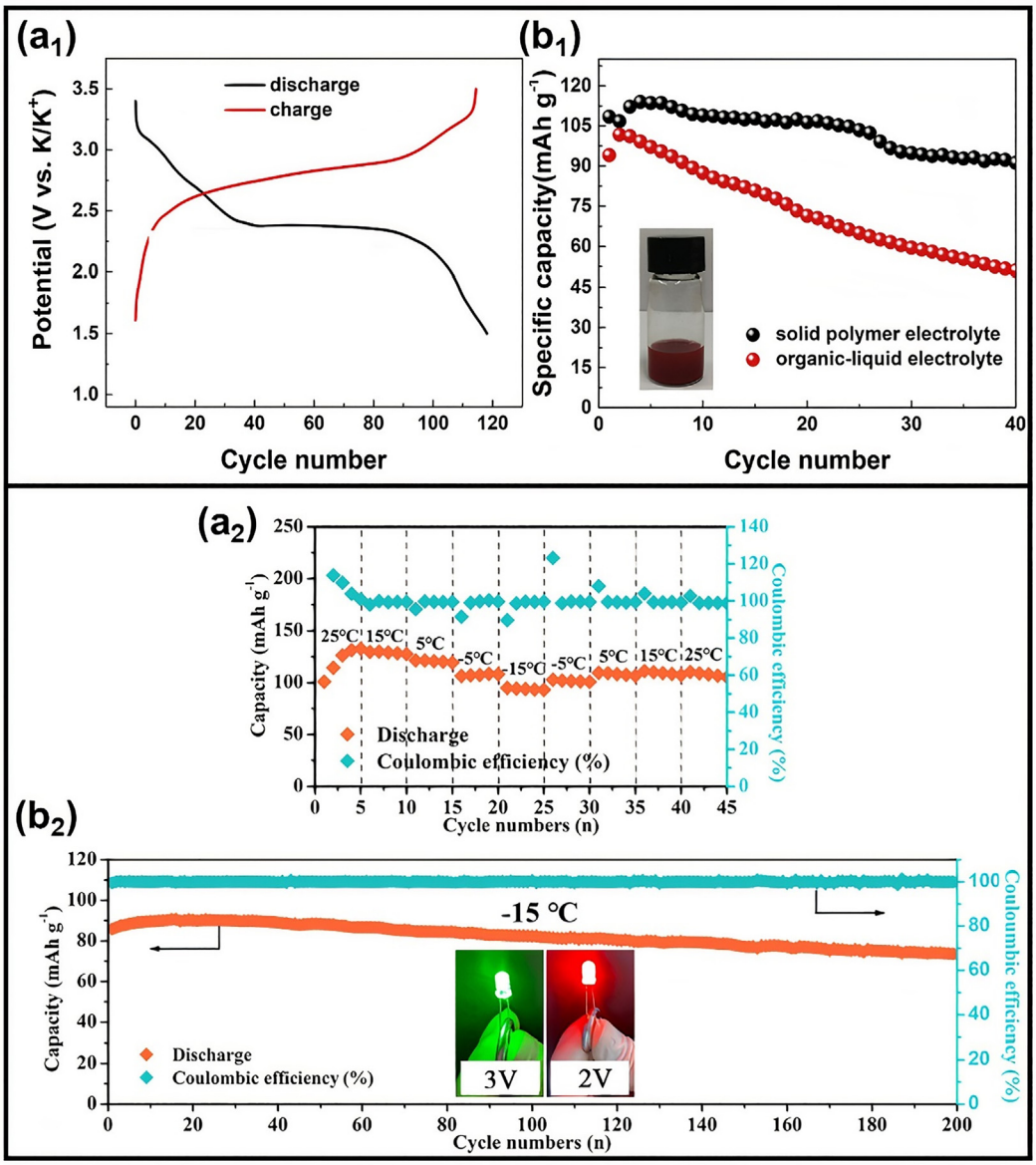

Fig. 5. (a_1) Charge/discharge profiles of PTCDA with PPCB-SPE at a current density of 10 mA g^{-1}. (b_1) Cycling performance of PTCDA with PPCB-SPE or organic-liquid electrolyte at a current density of 20 mA g^{-1}. The inserted digital image is the solubility test of PTCDA in 1 M KFSI in EC/DEC (*v*/*v*, 1:1) electrolyte. Reproduced with permission from Ref. [62]. Copyright 2018, Elsevier. (a_2) Cycling performance at different temperature and (b_2) capacity vs. cycle number of PCTDA || PFSA-K || Graphite full-cell at −15 °C. Reproduced with permission from Ref. [58]. Copyright 2021, Elsevier.

at 20 °C. The PTCDA cathode in the all-solid-state battery demonstrated a working discharge voltage of 2.3 V, an initial high capacity of 118 mA h g^{-1} at 10 mA g^{-1} (Fig. 5a1), and over 40 cycles, the cell retained 84% of its initial capacity (Fig. 5b1). At the opposite, the cell with organic-liquid electrolyte (KFSI based-electrolyte) presented a significant capacity fading of 45.7%, likely due to the high solubility of PTCDA into the organic-liquid electrolyte. This highlights the crucial advantage of using all-solid-state electrolytes in the case of organic electrodes and underlines the potential for further investigations. In the subsequent year, the same group designed a Ni_3S_2@Ni electrode for KIBs with a poly(ethylene oxide)-bis(flourosulfonyl)imide (PEO-KFSI)-based hybrid electrolyte, which exhibited an ionic conductivity of up to 2.7×10^{-4} S cm^{-1} at 60 °C [63]. The electrochemical performance of the solid-state KIBs revealed a high capacity of 312 mA h g^{-1} with a high CE of 97% during the first discharge process. The high CE can be attributed, in part, to the less solid electrolyte interphase growth. In 2021, Du et al. [58] introduced a novel approach to prepare polymer-based hybrid electrolyte membranes as quasi solid-state electrolytes using perfluorinated sulfonic resin powder (referred to as PFSA-K membrane). This method represents the first-ever development of such membranes for low-operating temperature of a KIB system. The PFSA-K membranes exhibit promising ionic conductivity across a wide temperature range from −15 to 85 °C, as well as excellent electrochemical stability and high mechanical flexibility. The synthesized electrolyte demonstrates good mechanical flexibility, outstanding electrochemical stability, and high ionic conductivity of 9.31×10^{-5} S cm^{-1} at 25 °C. Commercial raw materials, namely PTCDA and graphite were used as the cathode and anode materials to assemble the first quasi solid-state KIB cell, which exhibits excellent performance at low temperatures, with a reversible capacity of 94.8 mA h g^{-1} even at −15 °C. Upon returning to 25 °C, the initial capacity was recovered (Fig. 5a2). The cycling performance at −15 °C and 100 mA g^{-1} shows a capacity

retention of 85% over 200 cycles (Fig. 5b2), with an average CE close to 100%, indicating the stability and practicality of the PFSA-K membrane as quasi-solid-state electrolyte for KIBs operating at low temperatures. These results confirm the great potential for further commercialization.

4. Improvement strategies for innovative KIFCs

The previously mentioned achievements suggest that KIFCs have the potential to play a crucial role in the energy storage landscape, offering a sustainable and efficient solution for a range of applications, from portable electronic devices to grid energy storage. However, despite these remarkable advancements, several challenges still need to be overcome to fully achieve efficient and reliable KIBs as discussed thereafter. Thus, the following subsections will address the main strategies to improve further KIFCs with: (i) the optimization of electrolytes in regards to the SEI layers formation and thus the capacity retention (i.e. lifetime) improvement; (ii) the screening of electrodes materials in regards to the power and/or energy applications; (iii) a guideline regarding the assembly of liquid based KIFC so that highly reliable cells are obtained and (iv) others strategies to further unlock the full potential of KIBs.

4.1. Optimizing electrolytes to enable stable passivation layers

Anodes and cathodes working at lower and higher voltages are commonly used to develop cells with higher energy. However, this often leads to higher electrolyte side reactions and the formation of thicker SEI films with higher impedance, thus lowering the overall cells performance. Fig. 6(a) depicts that nonaqueous liquid electrolytes for KIFCs are classified into three categories: esters, ethers, and ionic liquids. It can be observed that ester-based electrolytes are the most used in KIFCs and are usually binary solvent systems. Although ethers exhibit good compatibility with most anodes, their susceptibility to oxidation at high voltages makes them rarely used in full-cells so far [64–66]. Ionic liquids offer higher safety and can operate over a wide temperature range, but their high viscosity, low ion mobility, and high cost limit their further application [67,68].

The ionic conductivity of the liquid electrolyte is closely related to the solvent's viscosity and dielectric constant. An ideal electrolyte should have high ionic conductivity, low viscosity, and sufficient high dielectric constant. Unfortunately, many solvents exhibit a mutual correlation between these parameters, so they are often used in combination with other solvents. The most commonly used solvents in current full-cells are EC, PC and DEC solvents (Fig. 6d), which often leads to poor cycle stability and should be used in combination with other solvents or additives. Linear carbonates exhibit lower viscosities and lower dielectric constants, but they usually involve poor electrochemical performance when used alone. Thus, they are often used as auxiliary solvents for the above two solvents (EC and PC) to enhance the overall performance of the electrolyte, and SEI stability [65]. Overall, the most commonly used solvents composition is EC:DEC.

The electrolyte salt type (Fig. 6c) is also an important factor to control the electrochemical performance (ionic conductivity, solvation/desolvation energy) and SEI formation. KPF_6 is the most commonly utilized electrolyte salt in KIFCs. It has moderate solubility in esters and the PF_6^- anions provide a passivation effect on the aluminium current collector. KPF_6-based electrolytes have been extensively studies and used in K-ion batteries [12,69]. However, the drawback of KPF_6-based electrolytes is that they tend to form an unstable SEI mostly based on organic solvent degradation products (in carbonates) on the anode surface as demonstrated so far in a half-cell using the highly reactive K metal [8,18,42]. Thus, most KPF_6-based electrolytes have low CE due to insufficient SEI passivation. On the other hand, KFSI-based electrolytes have also been studied, owing to their stable SEI growth (based mostly on KFSI degradation products in carbonates as observed in half-cells studies so far), resulting in low irreversible capacity and stable CE evolution upon electrochemical cycling. In contrast, they suffer from several issues, especially corrosion of the aluminium (Al) current collector at moderate and high voltages [52]. So, one possible solution to the Al corrosion issue is to utilize highly concentrated KFSI electrolytes (as illustrated in Fig. 7) along with KFSI-containing ionic liquids [12,51,70]. Nonetheless, KPF_6-KFSI binary salt electrolyte with a suitable salts ratio can overcome this challenge, leading to both effective Al passivation and high CE (as depicted in Fig. 7) [52]. This approach resolves the dilemma and offers a promising way forward.

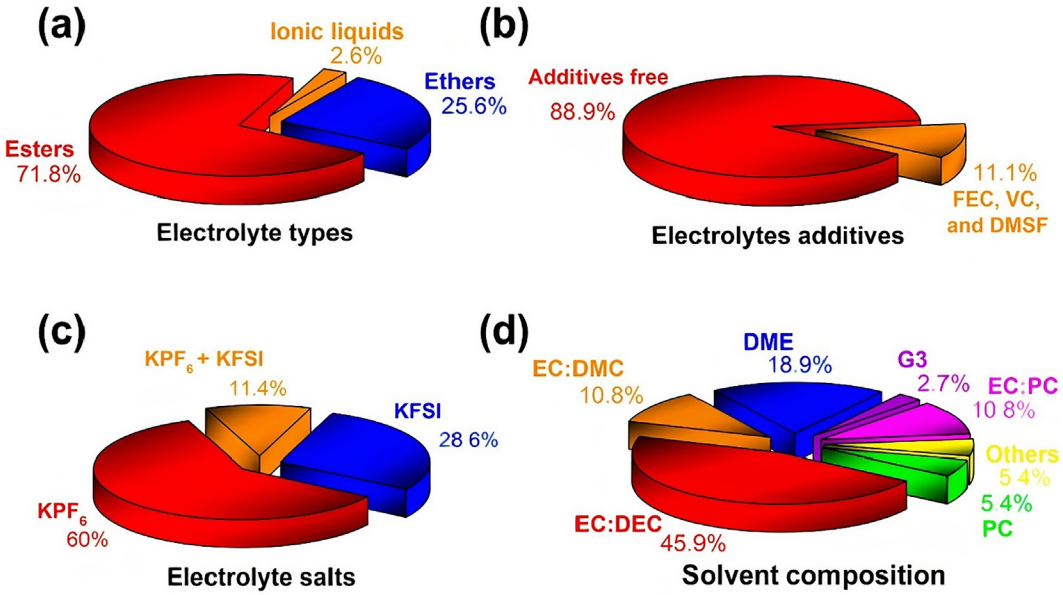

Fig. 6. Summary for the distribution of electrolyte (a) types, (b) additives, (c) salts, and (d) solvent composition in KIFCs.

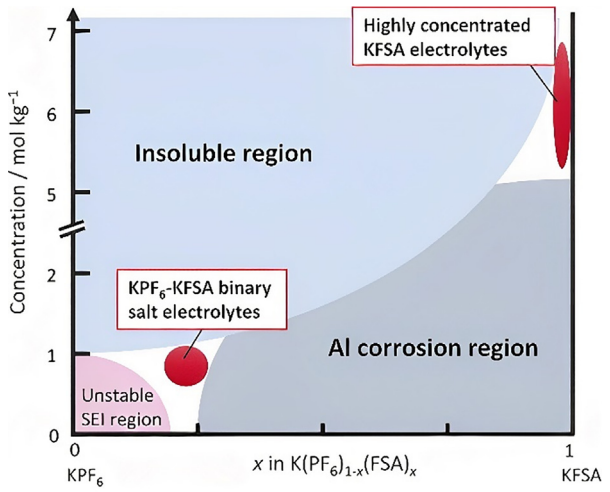

Fig. 7. Diagram of binary KPF_6-KFSI (in the diagram, KFSA stands for KFSI) salts ratio and concentration as function of corrosion, solubility, and SEI stability region. Reproduced with permission from Ref. [66]. Copyright 2022, Chemical Society of Japan.

Regarding additives, it is evident that this is a barely explored aspect in K-ion batteries (i.e. 88.9% of studies do not address additives), as shown in Fig. 6(d). To date, the majority of existing studies on additives in KIBs have been conducted in half-cell configuration rather than in full-cell, impacting the potassium metal SEI [8,71]. The observed electrochemical improvements may come from stabilizing the SEI of the potassium metal rather than the interface of the studied material. Consequently, electrolyte studies need to be conducted in a full-cell configuration for a comprehensive understanding.

In summary, the development of efficient and reliable nonaqueous electrolytes for K-ion batteries still faces numerous challenges. Future research should focus on the following aspects. Firstly, the formation mechanism and charge transfer of the SEI layer for full K-ion batteries are still not well explored, and more investigation is rapidly needed. Advanced in situ characterization methods, including in situ and operando analysis techniques, as well as theoretical simulations [72] can be used to explore further the reaction mechanism, crosstalk phenomenon [73], and microstructure of the electrode/electrolyte interface. Secondly, efforts should be made to reduce or control side reactions at high voltage. Although concentrated electrolytes can regulate polarization and reduce side reactions by solvation effects, their oxide-resistant properties at high potential should also be considered [53]. While KFSI-based electrolytes have been widely studied for their ability to make stable interfaces, their tendency to corrode the collector at high potential should be considered. Therefore, it is necessary to develop a more suitable new-type K-salt system, such as binary-salts, that can build a stable interface and avoid collector corrosion simultaneously. As the chemistry of electrolytes and their associated electrode/electrolyte interface continue to develop, we are confident that K-ion batteries with high energy density (and thus with relatively high voltage), low cost are possible.

4.2. Screening electrode materials for power and/or energy applications

At present, most of the work on KIFCs is based on nonaqueous liquid electrolytes. As illustrated in Fig. 8, among these reported KIFCs, the most prevalent positive electrode materials are PBAs (Prussian Blue Analogues) compounds followed by organics, while carbonaceous materials are the mainstream in negative electrodes materials [55,74–76].

Regarding anodes materials, graphite has demonstrated reasonable electrochemical performance when appropriate binders and electrolytes are used. Although other carbon forms have been shown to intercalate K ions, they are unlikely to be as effective as graphite in terms of energy (i.e. hard and soft carbons present a higher average potential and lower electrode density compared to graphite) [77]. Alloying anodes may not be a suitable choice for KIBs, as the same issues that affect them (i.e. huge volume expansion, and rapid capacity degradation) in LIBs and NIBs are worsened in KIBs, resulting in a significantly reduced energy density [78]. However, Gu et al. [79] explores enhancing the performance of the Alloy CoSe anode material by introducing a flexibly designed core–shell structure (CoSe–C@C) and promoting an SEI rich in inorganic compounds. The CoSe–C@C electrode shows remarkable stability, maintaining a high capacity of 432 mA h g^{-1} at 200 mA g^{-1} over 1000 cycles and demonstrating high rate capability (233 mA h g^{-1} at 10 A g^{-1}). On the other hand, intercalation oxide and phosphate materials have been shown to be stable for long-term cycling (i.e. $K_2Ti_4O_9$, $K_2Ti_8O_{17}$, and $KTi_2(PO_4)_3$), in contrast candidates with higher capacity and low average voltage are still needed [80–82]. Finally, conversion and organic molecules as anode materials are still in the early stages of development and require further evaluation for practical application. Hence, to advance the practical application in KIFCs and achieve enhanced performance, there is a need for further research and investigation into carbonaceous negative electrodes (i.e. composition, doping, and optimization of the electrode formulation process).

In the range of positive electrode materials for K-ion batteries, various types have been explored, each with its own set of advantages and drawbacks. Organic materials, such as small organic molecules, polymers, and organometallic complexes offer the benefits of low cost and reduced energy consumption during synthesis. However, they require an additional pre-potassiation step before use. Although organic cathode materials like perylene-3,4,9,10-tetracarboxylic dianhydride (PTCDA) and polyanthraquinone sulfide (PAQS) exhibit high capacity, they face challenges such as the need for annealing to improve electronic conductivity, slow ion migration, dissolution issues at high current densities, and low electronic

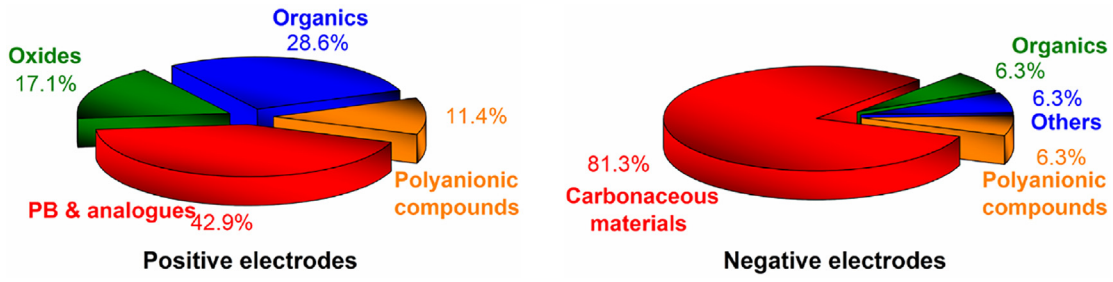

Fig. 8. Distribution summary of different electrodes materials in KIFCs (PB stands for Prussian blue).

conductivity [83,84]. Nonetheless, organic materials still hold potential for high capacity and good cycling performance for grid applications. Layered oxides, known for their high energy density, are commonly used as cathodes in Li-ion batteries and Na-ion batteries [85]. They have a 2D framework where transition metals and alkali ions are arranged in alternating blocks, facilitating rapid alkali ion migration. Various layered oxides have been developed for K-ion batteries, including $K_{0.3}MnO_2$ [86], P3-type $K_{0.5}MnO_2$ [87], and P2- and P3-type K_xCoO_2 [88]. However, layered K-compounds exhibit a low working potential, steeper voltage curves, and more voltage steps compared to Li and Na systems due to long-ranged repulsive interactions between alkali ions [89]. Additionally, the inherent structural instability of layered oxides limits their maximum allowable voltage, leading to capacity decay during overcharge [90]. Structural alteration upon depotassiation further restricts the range of K de/intercalation. Overcoming these limitations requires further investigation.PBAs have gained attention for K-ion batteries. While their use is not based on the performance of their Li counterparts, they offer stability, high ionic diffusion coefficient, and working potentials that exceed those of LIBs [91]. The electrochemical performance of PBA depends on chemical composition, morphology, particle size, and interstitial water content [29]. They display good performance at high current densities and have the potential for high capacity. However, their low-rate performance compared to polyanionic materials has limited their use from the power application point of view.

Polyanionic compounds, represented by $M_xT_y(XO_4)_z$ structures, exhibit good thermal and structural stability, operate at high potentials, and allow for rapid ion diffusion. However, they generally have low practical capacity, poor CE, and low electronic conductivity due to insulating groups between transition metals [92]. Notably, polyanionic compounds based on vanadium and phosphates or fluorophosphates have shown promising electrochemical properties for K-ion batteries. Various structures, including Tavorite compounds based on fluorophosphate and vanadium exhibit high operating potentials and theoretical energy densities comparable to $LiFePO_4$ [93]. For practical use, fluorophosphates (power applications) and PBAs (energy applications) demonstrate promising electrochemical performance with high working voltage, high-rate performance, and high structural stability. However, despite their potential, both fluorophosphates and PBAs require further improvement to address challenges such as capacity limitations, and low electronic conductivity. Continued research and development efforts are necessary to optimize their electrochemical properties and enable their practical application in full K-ion batteries.

To summarize, numerous studies have employed lamellar oxides as positive electrodes in K-ion batteries. However, these materials require enhancements due to their limited capacity and average voltage (i.e. new phases with more manganese and nickel). On the other hand, Prussian blue and its analogues have shown promise with their high capacity and average voltage. Yet, their water content remains a challenge that must be addressed to prevent catalytic reactions and safety concerns, especially at high voltage. Organic molecules used as cathode materials exhibit a combination of high capacity and low operating voltage. Nonetheless, there is route for improvement, particularly in mitigating the dissolution in organic electrolyte of these molecules and enhancing their density. Polyanionic frameworks as cathode materials offer advantages such as high power density and high average potential. However, their high anodic voltage limit, typically in the range of 4.5 to 5 volts, presents a challenge for conventional carbonate-based electrolytes, which struggle to resist such high potentials. In this context, the way of progress focuses on the electrolyte design, involving the strategic combination of additives (i.e. succinonitrile [94], vinylene carbonate [95], propene sulfone [96]) and materials design, which involves the doping [97], coating [92,98], and substitution [99]. Turning to the negative electrode side, graphite emerges as a promising candidate for KIFCs, but the volume expansion issue (approximately 60%) needs to be carefully addressed. Furthermore, a significant gap remains in the systematic research on electrolytes and their effects on KIFC performance, especially in terms of safety considerations. Additionally, the low ionic conductivity of organic-based electrolytes at room temperature presents a limitation that could be addressed using solid-state based electrolytes.

4.3. Improving liquid KIFCs parameters: Guideline toward reliable cells

This subsection aims to eliminate the need for electrochemical pre-cycling of electrodes prior to full-cell assembly, paving the way for the development of reliable KIFC configurations.

A full-cell optimization guideline was recently published, focusing on evaluation of different parameters for practical K-ion batteries assembly, as illustrated in Fig. 9 [23]. Due to their promising electrochemical performance, gaphite and $KVPO_4F_xO_{1-x}$ were chosen as active materials for the negative and positive electrodes, respectively. Note that another study have also previously addressed the challenge of graphite volume expansion by optimizing the electrode formulation (i.e. carbon additive content, binders choice and amount...), enhancing its potential as an electrode material [34]. Among the $KVPO_4F_xO_{1-x}$ family, $KVPO_4F_{0.5}O_{0.5}$ (KVPFO) exhibits the most favourable galvanostatic profile, showing lower polarization, smoother redox plateaus, improved reversible capacity, and CE [93].The full-cell optimization guideline study aimed at assessing the parameters impacting the performance of half-cells before assembling full-cells. To ensure accurate evaluation, precautions were taken during the preparation of K metal electrodes. The investigation highlights the importance of using a glass fiber separator on the K metal electrode side, due to its electrochemical instability when using Celgard or Solupor separators [23]. The choice of electrolyte also plays a crucial role, with 0.8 M KPF_6 EC: DEC exhibiting lower polarization versus K metal compared to other electrolytes tested. Interestingly, the volume of electrolyte, while often overlooked in literature, was found to significantly impact half-cells and full-cells performance. An optimal electrolyte volume of 70 μL was determined for both KVPFO and graphite half-cells, four times the total porosity of electrodes and separators. The impact of electrolyte volume on full-cell performance was also investigated. Increasing the electrolyte volume from 15 to 50 μL enhances capacity and CE while reducing polarization. However, further increasing the volume to 70 and 100 μL decreases capacity and CE, likely due to excessive electrolyte degradation and passivation of electrode surfaces by SEI. The optimal electrolyte volume for KVPFO//graphite cells was found to be 50 μL, four times the total porosity of electrodes and separators as for half-cells.

This study also examined the influence of the negative//positive (N/P) electrode diameter ratio on full-cell performance. Larger diameter ratios lead to increased irreversible capacity and polarization associated with electrolyte degradation. A N/P diameter ratio of 1.16 was found to provide optimal performance. Further investigation into the graphite//KVPFO capacity ratio reveals that a ratio of 1.16 provides the highest initial capacity, CE, capacity retention, and lowest polarization. Lower and higher ratios result in limitations involved by KVPFO and graphite electrodes, respectively.

Furthermore, pre-cycling the electrodes before battery assembly may offers an effective solution for the balancing challenges. However, this method encounters safety concerns and high expenses. Zhao et al. [100] presented a cost-effective and direct

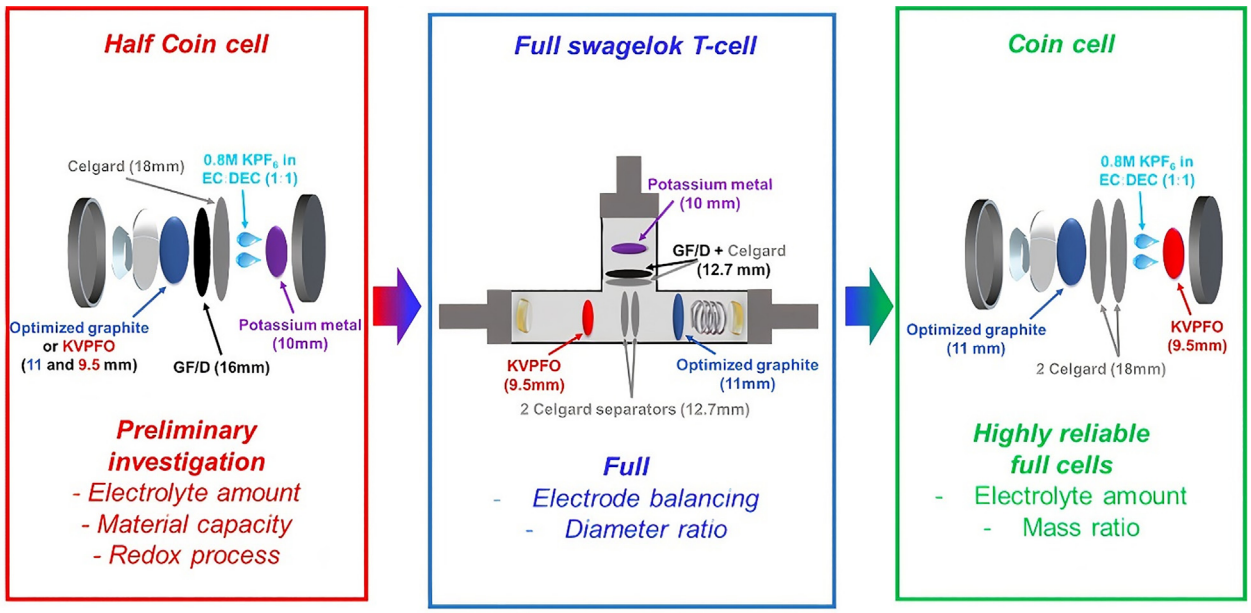

Fig. 9. Schematic representation of the method followed to optimize the assembly of highly reliable K-ion full coin cells. Reproduced with permission from Ref. [23]. Copyright 2023, Wiley-VCH.

approach to compensate for potassium deficiencies by using a self-sacrificial additives (i.e. as $K_2C_4O_4$) within positive electrode to enhance potassium-ion battery performance. Their findings demonstrate that incorporating $K_2C_4O_4$ into a P3-type $K_{0.5}MnO_2$ cathode remarkably elevates the initial coulombic efficiency from 53.6% to an unprecedented high of 93.5%.

Finally, the optimized N/P diameter and capacity ratios were applied to assemble high-loading KVPFO//graphite coin cells (4 mg cm^{-2} for graphite and 10 mg cm^{-2} for KVPFO). The study achieves an energy density of approximately 47 W h kg^{-1}_{device} with 68% capacity retention after 20 cycles, representing probably the highest reported energy densities for KIBs, especially considering the high active material mass loadings. Thus, with optimized electrode formulation and practical electrolyte volume, pouch cells could potentially reach an energy density of around 80 W h kg^{-1}. These findings thus highlight the importance of electrode material selection, electrolyte choice, electrolyte volume, electrode surface ratio, and electrode areal capacity ratio in optimizing the performance of KIFCs and also importantly their reliability, thus paving the way for their potential application as high-energy density storage systems.

Furthermore, the analysis of solid electrolyte interphase and cathode electrolyte interface in full-cell configurations requires more investigations due to the superior reliability of results and the circumvention of K metal cross-talk species compared to half-cell studies. Notably, the SEI and CEI layers in full-cell setups were found to be notably thinner, measuring less than 5 Å [101], as opposed to the substantially thicker layers exceeding 10 Å observed in half-cell configurations [26]. This distinction underscores the heightened relevance of investigating these interfaces within full-cell configuration.

Moreover, Larhrib et al. showed an insightful exploration into the SEI and CEI growth and aging in KVPFO/graphite full-cells. As summarized in Fig. 10, their investigation shed light on critical findings. (i) Open circuit voltage (OCV) temperature influence: Higher OCV temperatures, particularly at 40 °C for 12 h, resulted in a pronounced inorganic passivation layer. This enhancement potentially improves electrode wetting by electrolyte, correlating with better electrochemical performance compared to other temperatures. (ii) Upper cut-off voltage (UCV) optimization: An optimal UCV of 4.8 demonstrated a balanced formation between organic and inorganic passivation layers, leading to improved capacity retention and coulombic efficiency evolution, unlike the UCVs of 4.5 and 5 V UCVs. (iii) Depth of discharge (DOD) impact: SEI dissolution was observed to be higher at 1.2 V DOD, resulting in a thinner SEI. An SEI inorganic/organic species ratio close to 1 at 2.0 V DOD suggested a more stable passivation layer (more KF, K_2CO_3, and KPF_6 decomposition species), contributing to better electrochemical performance. (iv) Vanadium dissolution: In the graphite/KVPFO full-cell, capacity loss was attributed partly to vanadium dissolution initiated from the first cycle. (v) Effect of DOD on rate performance: Higher DOD at 1.2 V showed lower capacity at high rates, indicating increased impedance (i.e. Different SEI and CEI aging mechanisms). In contrast, 2 V DOD exhibited higher capacity at high rates.

Thus, the comprehensive exploration of SEI and CEI analysis within potassium-ion full-cells reveals a wealth of insights crucial for advancing this energy storage technology. However, to truly control the potential of KIBs and translate these insights into practical applications, the next pivotal step is the transition toward prototyping KIBs. Through prototyping efforts, we can bridge the gap between academic and industrial implementation, driving KIBs toward their full potential in the landscape of energy storage solutions.

Likewise, as a proof of concept, the electrochemical performance of KIFCs should be investigated preferably in pouch and 18,650 cells format to demonstrate their practical interest. Fig. 11 presents a brief history of the pouch cell studied in K-ion technology so far with the surface area of the cells and their capacity when available. For instance, the design of a stackable PTCDA||KC_8 pouch cell provides the highest obtained capacity for KIBs [102] with106 mA h $g^{-1}_{cathode}$. PTCDA||KC_8 pouch cells consisted in 3-layer PTCDA cathodes (7 cm × 11 cm) sandwiched by 2-layers KC_8 foils (7 cm × 11 cm). Moreover, the cell demonstrates a capacity retention of 84.1% even after 100 cycles, indicating its long-term performance. Moreover, it is worth noting that there have been no research articles published so far regarding cylindrical 18,650 cells in KIBs, in contrast to the extensive research conducted on Na and

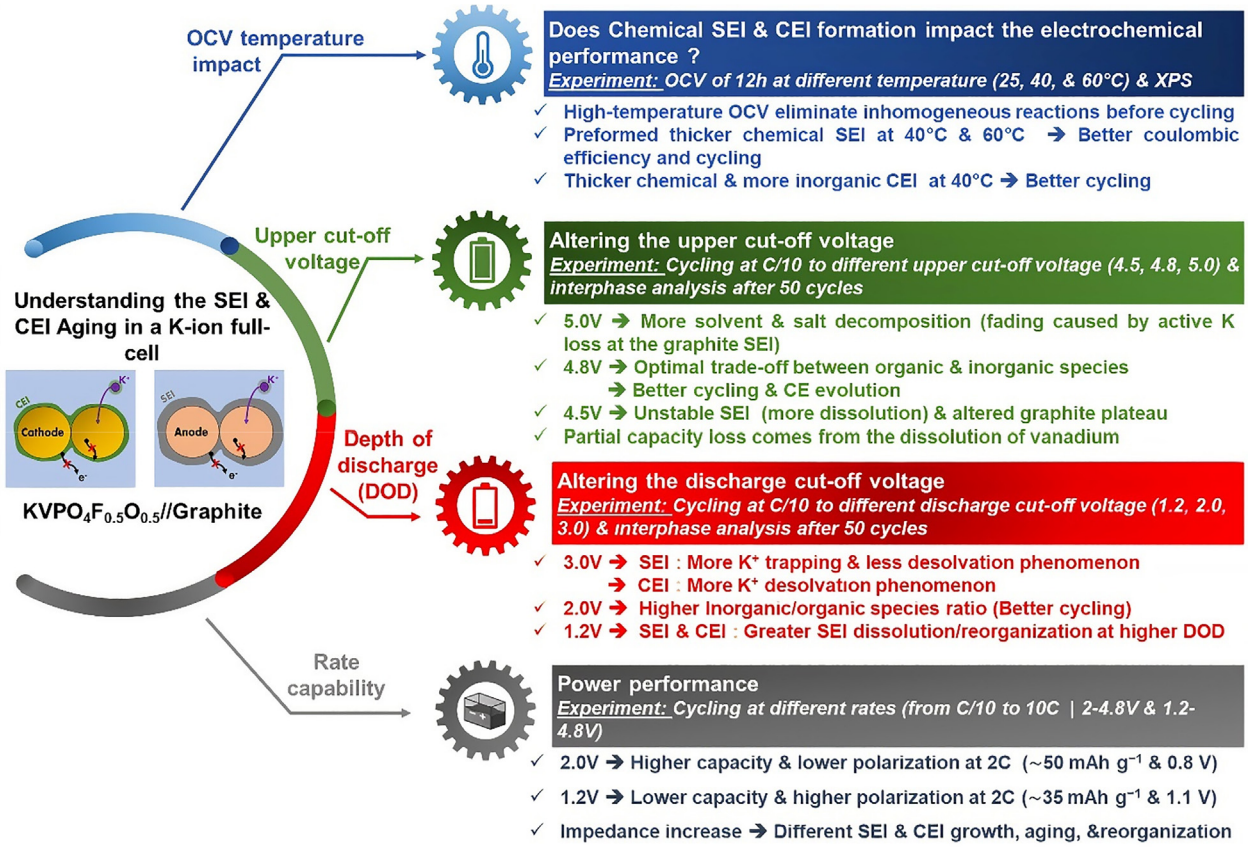

Fig. 10. Summary scheme illustrating the main results obtained from SEI and CEI growth/aging in the $KVPO_4F_{0.5}O_{0.5}$//Graphite full-cell configuration [101].

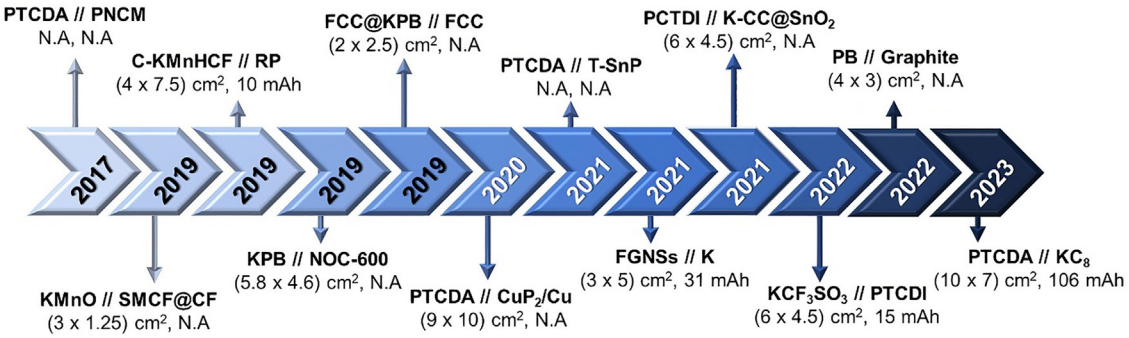

Fig. 11. A brief history of K-ion pouch cells (cathode//anode materials, (width × length) of the pouch cell, cell capacity, and N.A stands for Not Available). N-doped porous carbon monolith (PNCM) [45], $K_{0.3}MnO_2$ (KMnO) and self-supporting carbon nanotubes encapsulated in submicro carbon fiber (SMCF@CNTs) [105], potassium manganese hexacyanoferrate (KMnHCF) and red Phosphorus (RP) [106], potassium Prussian blue (KPB) and nitrogen/oxygen co-doped amorphous carbon (NOC-600) [107], flexible carbon cloth (FCC) and KPB [108], copper nanowires (CuP_2/Cu NWs) and PTCDA [109], $SnP_{0.94}$ teardrop nanorods (T-SnP) and PTCDA [110], K metal and fluorinated graphite nanosheets (FGNSs) [111], PTCDI and K metal on SnO_2-modified commercial carbon cloth (K-CC@SnO_2) [112], KCF_3SO_3 and PTCDI [113], graphite and Prussian blue (PB) [114], PTCDA and potassiated graphite (KC_8) [102].

Li technologies [103,104]. Exploring the potential of cylindrical 18,650 cells is of utmost importance for the advancement of K-ion technology, as it would provide valuable insights into their applicability and practicality.

4.4. Other strategies

In the existing literature, only a limited number of papers have addressed the topic of electrode formulation and design, which was crucial in the advancement of Li- and Na-ion batteries [115–120]. Regarding KIBs, it has been observed that the use of polytetrafluoroethylene (PTFE) as a binder for PBA positive electrodes offers advantages due to the formation of a more stable solid electrolyte interphase compared to polyvinylidene fluoride (PVDF) [52] despite that for practical use PVDF is more suitable. For the negative electrode, it has been demonstrated that the use of CMC as a binder yields high ICE, low polarization, and stable SEI growth compared to sodium polyacrylate (PANa) and PVDF [52,121]. This outcome has been confirmed by a recently published study, which highlights the impact of the binder in terms of electrochemical performance of graphite electrode [34]. This study showcased that the use of a binary binder comprising CMC and styrene-butadiene rubber (SBR) enhances several aspects, including volume expansion management, cohesion between the active material (graphite), car-

bon black, and binders, along with the overall electrochemical performance (i.e. rate performance, polarization, CE, and capacity). The electrode composition plays a crucial role in determining the energy density of a battery. Achieving a high loading of active materials in the electrodes while minimizing the use of carbon blacks and binders is essential to optimize the electrochemical performance. However, striking a balance between these parameters is necessary to achieve the best overall performance. Thus, the consideration of composition and formulation processes is crucial and needs increased focus. More importantly, as the electrode formulation plays a critical role in the overall materials performance, it should be a prerequisite for any new materials performance evaluation in the future. Similarly, increasing the active mass loading to a minimum range of 3–5 mg/cm^2 should also be a prerequisite to really investigate the practical performance of new materials. Overall, these aspects provide key factors in advancing the commercialization of KIBs.

5. Conclusions and outlook

Although potassium-ion batteries exhibit slow dynamics compared with Li-ion batteries and Na-ion batteries, the abundant resource and low cost endow KIBs to be the ideal candidate for large-scale energy storage systems. Research interest for K-ion full-cells has rapidly increased. Many novel KIFCs have been reported recently in the literature. This review summarizes the current status and prospects of potassium-ion full-cells. By studying and understanding the key issues including, K metal cross-talk issues, interfaces, the selection of appropriate electrode materials and proper electrolyte will remedy the K metal reactivity challenges and promote the use of KIFCs for large-scale energy storage applications. We have shown throughout this review that KIFCs are generally categorized into three main groups: liquid KIFCs, quasi- and all-solid-state KIFCs. Depending of the cell-type, it allow achieving high structural stability in a wide range of temperature and voltage. Giving more attention to the KIFCs will contribute to the advancement of KIBs industrialization because of the significant difference in electrochemical performance between half- and full-cells. As an advisory, more attention should be paid to KIFCs in the future research such as evaluating electrode materials, electrolytes, and so on. Furthermore, improving the initial coulombic efficiency is the key to enable the full electrochemical performance of KIFCs without pre-cycling the electrodes versus K metal. Moreover, KIFCs are the most widely studied and most promising KIB technology. Currently, its specific capacity can reach 104 mA h g^{-1} based on the mass of cathode and an average voltage of 3.9 V. However, its long-term cycle stability needs to be improved further by playing with the electrode material interface the electrolytes optimization and electrode design, as well as material engineering (coating, doping, and so on) [122,123]. Thanks to more stable interface characteristics, the quasi and all-solid-state KIFCs can exhibit better cycle durability than liquid ones when organic cathodes are used. However, few reports are obviously not conductive to its rapid progress, so it is expected to receive more attention based on its own superiority. The all-solid-state KIFCs with high voltage stability and safety can enable the potential of higher voltage materials to be fully utilized and thus achieve significant increase in energy densities. Notably, in place of the irreversible consumption of potassium ions, the electrode/electrolyte and electrolyte/electrolyte interface impedance in all-solid-state cells are the key factors that restrict their dynamic behaviours, thus their cycle stability and capacity at room temperature are often unsatisfactory. Generally, among the three types of full-cells, the all-solid-state ones still have a long way to go. How to manipulate effectively the solid–solid interface is the tipping point to realize its practical use toward the high-energy density.

Energy density, as a key indicator to evaluate the overall KIFCs performance, is primarily affected by operating voltage, capacity, materials tap density, cell design, and coulombic efficiency. Therefore, to obtain the targeted energy density, KIFCs need to be further investigated while the capacity ratio of cathode/anode must be strictly controlled. Irreversible consumption of K^+ ions is inevitable in a cell due to the presence of SEI and CEI growths and cross-talk. To compensate for these losses, novel strategies should be studied, most importantly the electrolyte formulation that have been neglected so far. Constrained by the previously mentioned issues, the cost/performance compromise and safety issues faced by this technology will be the biggest barrier toward the first efficient KIFCs prototype. Indeed, there is a lack of research articles on the use of cylindrical 18,650 cells in KIFCs compared to the extensive research on sodium and lithium technologies. However, it is crucial to investigate the potential of both pouch and cylindrical 18,650 cells in KIBs as it would offer valuable insights into their feasibility and practical use. Overall, in the current research of KIFCs, comprehensively examining the performance of KIFCs from the perspective of various mentioned gaps is critical for accelerating its progress.

Declaration of competing interest

The authors declare that they have no known competing financial interests or personal relationships that could have appeared to influence the work reported in this paper.

Acknowledgments

This work was supported by the Agence Nationale de la Recherche, France (ANR) through the TROPIC project (ANR-19-CE05-0026).

Appendix A. Supplementary material

Supplementary material to this article can be found online at https://doi.org/10.1016/j.jechem.2024.01.033.

References

[1] T. Hosaka, K. Kubota, A.S. Hameed, S. Komaba, Chem. Rev. 120 (2020) 6358–6466.
[2] E. Olsson, J. Yu, H. Zhang, H.-M. Cheng, Q. Cai, Adv. Energy Mater. 12 (2022) 2200662.
[3] S. Komaba, T. Hasegawa, M. Dahbi, K. Kubota, Electrochem. Commun. 60 (2015) 172–175.
[4] Y. Liu, C. Gao, L. Dai, Q. Deng, L. Wang, J. Luo, S. Liu, N. Hu, Small. 16 (2020) 2004096.
[5] H. Yin, C. Han, Q. Liu, F. Wu, F. Zhang, Y. Tang, Small. 17 (2021) 2006627.
[6] M. Patel, K. Mishra, R. Banerjee, J. Chaudhari, D.K. Kanchan, D. Kumar, J. Energy Chem. 81 (2023) 221–259.
[7] X. Chen, Y.-K. Bai, X. Shen, H.-J. Peng, Q. Zhang, J. Energy Chem. 51 (2020) 1–6.
[8] L. Caracciolo, L. Madec, G. Gachot, H. Martinez, ACS Appl. Mater. Interfaces. 13 (2021) 57505–57513.
[9] N. Xiao, W.D. McCulloch, Y. Wu, J. Am. Chem. Soc. 139 (2017) 9475–9478.
[10] K. Kubota, M. Dahbi, T. Hosaka, S. Kumakura, S. Komaba, Chem. Record 18 (2018) 459–479.
[11] J. Touja, V. Gabaudan, F. Farina, S. Cavaliere, L. Caracciolo, L. Madec, H. Martinez, A. Boulaoued, J. Wallenstein, P. Johansson, L. Stievano, L. Monconduit, Electrochim. Acta. 362 (2020) 137125.
[12] T. Hosaka, K. Kubota, H. Kojima, S. Komaba, Chem. Commun. 54 (2018) 8387–8390.
[13] J. Xie, J. Li, W. Zhuo, W. Mai, Mater. Today Adv. 6 (2020) 100035.
[14] Q. Li, Y. Wang, X. Wang, X. Sun, J.-N. Zhang, X. Yu, H. Li, ACS Appl. Mater. Interfaces. 12 (2020) 2319–2326.
[15] T.J. Lee, H. Kim, H.S. Hwang, J. Soon, J. Jung, J.H. Ryu, S.M. Oh, J. Electrochem. Soc. 165 (2018) A575.
[16] J. Zhang, Z. Cao, L. Zhou, G.-T. Park, L. Cavallo, L. Wang, H.N. Alshareef, Y.-K. Sun, J. Ming, ACS Energy Lett. 5 (2020) 3124–3131.

[17] Q. Li, Z. Cao, W. Wahyudi, G. Liu, G.-T. Park, L. Cavallo, T.D. Anthopoulos, L. Wang, Y.-K. Sun, H.N. Alshareef, J. Ming, ACS Energy Lett. 6 (2021) 69–78.
[18] L. Madec, V. Gabaudan, G. Gachot, L. Stievano, L. Monconduit, H. Martinez, ACS Appl. Mater. Interfaces 10 (2018) 34116–34122.
[19] F. Allgayer, J. Maibach, F. Jeschull, ACS Appl. Energy Mater. 5 (2022) 1136–1148.
[20] H. Wang, D. Zhai, F. Kang, Energy Environ. Sci. 13 (2020) 4583–4608.
[21] F. Yuan, Z. Li, D. Zhang, Q. Wang, H. Wang, H. Sun, Q. Yu, W. Wang, B. Wang, Adv. Sci. 9 (2022) 2200683.
[22] H. Aziam, B. Larhrib, C. Hakim, N. Sabi, H. Ben Youcef, I. Saadoune, Renew. Sustain. Energy Rev. 167 (2022) 112694.
[23] B. Larhrib, L. Madec, Batteries Supercaps. 6 (2023) e202300061.
[24] E. Pargoletti, S. Arnaboldi, G. Cappelletti, M. Longhi, D. Meroni, A. Minguzzi, P. R. Mussini, S. Rondinini, A. Vertova, Electrochim. Acta. 415 (2022) 140258.
[25] S.S. Zhang, J. Power Sources 164 (2007) 351–364.
[26] A.J. Naylor, M. Carboni, M. Valvo, R. Younesi, ACS Appl. Mater. Interfaces. 11 (2019) 45636–45645.
[27] D. Djian, F. Alloin, S. Martinet, H. Lignier, J. Power Sources 187 (2009) 575–580.
[28] W. Zhang, Y. Liu, Z. Guo, Sci. Adv. 5 (2019) eaav7412.
[29] S. Dhir, S. Wheeler, I. Capone, M. Pasta, Chem. 6 (2020) 2442–2460.
[30] L.-F. Zhao, Z. Hu, W.-H. Lai, Y. Tao, J. Peng, Z.-C. Miao, Y.-X. Wang, S.-L. Chou, H.-K. Liu, S.-X. Dou, Adv. Energy Mater. 11 (2021) 2002704.
[31] G. Guzmán, J. Vazquez-Arenas, G. Ramos-Sánchez, M. Bautista-Ramírez, I. González, Electrochim. Acta. 247 (2017) 451–459.
[32] H.-C. Wu, H.-C. Wu, E. Lee, N.-L. Wu, Electrochem. Commun. 12 (2010) 488–491.
[33] H.J. Kim, N. Voronina, H. Yashiro, S.-T. Myung, ACS Appl. Mater. Interfaces. 12 (2020) 42723–42733.
[34] B. Larhrib, L. Madec, L. Monconduit, H. Martinez, Electrochim. Acta. 425 (2022) 140747.
[35] H.-J. Liang, Z.-Y. Gu, X.-Y. Zheng, W.-H. Li, L.-Y. Zhu, Z.-H. Sun, Y.-F. Meng, H.-Y. Yu, X.-K. Hou, X.-L. Wu, J. Energy Chem. 59 (2021) 589–598.
[36] Z. Hong, H. Maleki, T. Ludwig, Y. Zhen, M. Wilhelm, D. Lee, K.-H. Kim, S. Mathur, J. Energy Chem. 62 (2021) 660–691.
[37] Y. Sun, F. Zeng, Y. Zhu, P. Lu, D. Yang, J. Energy Chem. 61 (2021) 531–552.
[38] Z. Xia, X. Chen, H. Ci, Z. Fan, Y. Yi, W. Yin, N. Wei, J. Cai, Y. Zhang, J. Sun, J. Energy Chem. 53 (2021) 155–162.
[39] T. Li, Q. Zhang, J. Energy Chem. 27 (2018) 373–374.
[40] H. Wang, H. Du, H. Zhang, S. Meng, Z. Lu, H. Jiang, C. Li, J. Wang, J. Energy Chem. 76 (2023) 67–74.
[41] Z. Yu, R. Li, K. Cai, Y. Yao, J. Deng, S. Lou, M. Lu, Q. Pan, G. Yin, Z. Jiang, J. Wang, J. Energy Chem. 58 (2021) 355–363.
[42] X. Bie, K. Kubota, T. Hosaka, K. Chihara, S. Komaba, J. Mater. Chem. A. 5 (2017) 4325–4330.
[43] X. Wang, K. Han, D. Qin, Q. Li, C. Wang, C. Niu, L. Mai, Nanoscale. 9 (2017) 18216–18222.
[44] H. Kim, J.C. Kim, S.-H. Bo, T. Shi, D.-H. Kwon, G. Ceder, Adv. Energy Mater. 7 (2017) 1700098.
[45] Y. Xie, Y. Chen, L. Liu, P. Tao, M. Fan, N. Xu, X. Shen, C. Yan, Adv. Mater. 29 (2017) 1702268.
[46] L. Zhang, B. Zhang, C. Wang, Y. Dou, Q. Zhang, Y. Liu, H. Gao, M. Al-Mamun, W. K. Pang, Z. Guo, S.X. Dou, H.K. Liu, Nano Energy. 60 (2019) 432–439.
[47] D. Li, W. Tang, C. Wang, C. Fan, Electrochem. Commun. 105 (2019) 106509.
[48] M. Xiong, W. Tang, B. Cao, C. Yang, C. Fan, J. Mater. Chem. A. 7 (2019) 20127–20131.
[49] J.-Y. Hwang, J. Kim, T.-Y. Yu, H.-G. Jung, J. Kim, K.-H. Kim, Y.-K. Sun, J. Mater. Chem. A. 7 (2019) 21362–21370.
[50] J.U. Choi, Y. Ji Park, J.H. Jo, Y.H. Jung, D.-C. Ahn, T.-Y. Jeon, K.-S. Lee, H. Kim, S. Lee, J. Kim, S.-T. Myung, Energy Storage Mater. 27 (2020) 342–351.
[51] H. Onuma, K. Kubota, S. Muratsubaki, T. Hosaka, R. Tatara, T. Yamamoto, K. Matsumoto, T. Nohira, R. Hagiwara, H. Oji, S. Yasuno, S. Komaba, ACS Energy Lett 5 (2020) 2849–2857.
[52] T. Hosaka, T. Matsuyama, K. Kubota, S. Yasuno, S. Komaba, ACS Appl. Mater. Interfaces 12 (2020) 34873–34881.
[53] T. Hosaka, T. Matsuyama, K. Kubota, R. Tatara, S. Komaba, J. Mater. Chem. A. 8 (2020) 23766–23771.
[54] Y. Wei, H. Wang, J. Wang, C. Gao, H. Zhang, F. Yuan, J. Dong, D. Zhai, F. Kang, ACS Appl. Mater. Interfaces. 13 (2021) 54079–54087.
[55] A. Li, L. Duan, J. Liao, J. Sun, Y. Man, X. Zhou, ACS Appl. Energy Mater. 5 (2022) 11789–11796.
[56] J. Zhao, Y. Qin, L. Li, H. Wu, X. Jia, X. Zhu, H. Zhao, Y. Su, S. Ding, Sci. Bull. 68 (2023) 593–602.
[57] S. Chen, J. Zhong, H. Deng, Q. Wei, X. Shen, X. Jia, S. Li, Q. Zhang, J. Zhu, B. Lu, W. Yang, CCS Chem. (2023) 1–13.
[58] G. Du, M. Tao, D. Liu, M.K. Aslam, Y. Qi, J. Jiang, Y. Li, S. Bao, M. Xu, J. Colloid Interface Sci. 582 (2021) 932–939.
[59] H. Liu, X.-B. Cheng, J.-Q. Huang, H. Yuan, Y. Lu, C. Yan, G.-L. Zhu, R. Xu, C.-Z. Zhao, L.-P. Hou, C. He, S. Kaskel, Q. Zhang, ACS Energy Lett. 5 (2020) 833–843.
[60] L. Li, Y. Deng, G. Chen, J. Energy Chem. 50 (2020) 154–177.
[61] R. Rajagopalan, Y. Tang, X. Ji, C. Jia, H. Wang, Adv. Func. Mater. 30 (2020) 1909486.
[62] H. Fei, Y. Liu, Y. An, X. Xu, G. Zeng, Y. Tian, L. Ci, B. Xi, S. Xiong, J. Feng, J. Power Sources 399 (2018) 294–298.
[63] H. Fei, Y. Liu, Y. An, X. Xu, J. Zhang, B. Xi, S. Xiong, J. Feng, J. Power Sources 433 (2019) 226697.
[64] C. Wang, W. Tang, X.L. Wang, Y.H. Zhou, D. Li, S. Jia, B. Cao, C. Fan, Electrochim. Acta. 365 (2021) 137365.
[65] Y.-B. Niu, Y.-X. Yin, Y.-G. Guo, Small. 15 (2019) 1900233.
[66] T. Hosaka, S. Komaba, BCSJ. 95 (2022) 569–581.
[67] H. Niu, L. Wang, P. Guan, N. Zhang, C. Yan, M. Ding, X. Guo, T. Huang, X. Hu, J. Energy Storage 40 (2021) 102659.
[68] B. Larhrib, G. Nikiforidis, M. Anouti, Electrochim. Acta. 371 (2021) 137841.
[69] W. Luo, J. Wan, B. Ozdemir, W. Bao, Y. Chen, J. Dai, H. Lin, Y. Xu, F. Gu, V. Barone, L. Hu, Nano Lett. 15 (2015) 7671–7677.
[70] M. Fiore, S. Wheeler, K. Hurlbutt, I. Capone, J. Fawdon, R. Ruffo, M. Pasta, Chem. Mater. 32 (2020) 7653–7661.
[71] J. Park, J. Lee, M.H. Alfaruqi, W.J. Kwak, J. Kim, J.Y. Hwang, Mater. Chem. A. 8 (2020) 16718–16737.
[72] X. Wang, H. Liu, K. Pan, R. Huang, X. Gou, Y. Qiang, J. Energy Storage 67 (2023) 107578.
[73] C. Li, X. Zhang, Z. Yang, H. Lv, T. Song, S. Lu, Y. Zhang, T. Yang, F. Xu, F. Wu, D. Mu, J. Energy Chem. 87 (2023) 342–350.
[74] S. Aldroubi, B. Larhrib, L. Larbi, I. Bou Malham, C. Matei Ghimbeu, L. Monconduit, A. Mehdi, N. Brun, J. Mater. Chem. A. 11 (2023) 16755–16766.
[75] L. Larbi, B. Larhrib, A. Beda, L. Madec, L. Monconduit, C. Matei Ghimbeu, ACS Appl. Energy Mater. 6 (2023) 5274–5289.
[76] M. Carboni, A.J. Naylor, M. Valvo, R. Younesi, RSC Adv. 9 (2019) 21070–21074.
[77] Z. Jian, S. Hwang, Z. Li, A.S. Hernandez, X. Wang, Z. Xing, D. Su, X. Ji, Adv. Func. Mater. 27 (2017) 1700324.
[78] W. Zhang, J. Mao, S. Li, Z. Chen, Z. Guo, J. Am. Chem. Soc. 139 (2017) 3316–3319.
[79] X. Gu, L. Zhang, W. Zhang, S. Liu, S. Wen, X. Mao, P. Dai, L. Li, D. Liu, X. Zhao, Z. Guo, J. Mater. Chem. A. 9 (2021) 11397–11404.
[80] B. Kishore, V.G.N. Munichandraiah, J. Electrochem. Soc. 163 (2016) A2551.
[81] J. Han, M. Xu, Y. Niu, G.-N. Li, M. Wang, Y. Zhang, M. Jia, C. ming Li, Chem. Commun. 52 (2016) 11274–11276.
[82] J. Han, Y. Niu, S. Bao, Y.-N. Yu, S.-Y. Lu, M. Xu, Chem. Commun. 52 (2016) 11661–11664.
[83] Y. Hu, W. Tang, Q. Yu, X. Wang, W. Liu, J. Hu, C. Fan, Adv. Func. Mater. 30 (2020) 2000675.
[84] M. Guo, W. Tang, C. Tang, X. He, J. Hu, C. Fan, ChemSusChem. 16 (2023) e202300343.
[85] P.K. Nayak, L. Yang, W. Brehm, P. Adelhelm, Angew. Chem. Int. Ed. 57 (2018) 102–120.
[86] C. Vaalma, G.A. Giffin, D. Buchholz, S. Passerini, J. Electrochem. Soc. 163 (2016) A1295.
[87] H. Kim, D.-H. Seo, J.C. Kim, S.-H. Bo, L. Liu, T. Shi, G. Ceder, Adv. Mater. 29 (2017) 1702480.
[88] Y. Hironaka, K. Kubota, S. Komaba, Chem. Commun. 53 (2017) 3693–3696.
[89] H. Kim, J.C. Kim, M. Bianchini, D.-H. Seo, J. Rodriguez-Garcia, G. Ceder, Adv. Energy Mater. 8 (2018) 1702384.
[90] M. Wang, H. Zhang, J. Cui, S. Yao, X. Shen, T.J. Park, J.-K. Kim, Energy Storage Mater. 39 (2021) 305–346.
[91] P.N.L. Pham, R. Wernert, M. Cahu, M. Tahar Sougrati, G. Aquilanti, P. Johansson, L. Monconduit, L. Stievano, J. Mater. Chem. A. 11 (2023) 3091–3104.
[92] L. Larbi, R. Wernert, P. Fioux, L. Croguennec, L. Monconduit, ACS Appl. Mater. Interfaces 15 (2023) 18992–19001.
[93] R. Wernert, L.H.B. Nguyen, E. Petit, P.S. Camacho, A. Iadecola, A. Longo, F. Fauth, L. Stievano, L. Monconduit, D. Carlier, L. Croguennec, Chem. Mater. 34 (2022) 4523–4535.
[94] H.S. Refai, N. Yacout, M. Farrag, S.Y. Ibrahim, M.A. Kebede, F. Salman, E. Sheha, J. Energy Storage 70 (2023) 107954.
[95] J. Shi, L. Ding, Y. Wan, L. Mi, L. Chen, D. Yang, Y. Hu, W. Chen, J. Energy Chem. 57 (2021) 650–655.
[96] L. Li, D. Wang, G. Xu, Q. Zhou, J. Ma, J. Zhang, A. Du, Z. Cui, X. Zhou, G. Cui, J. Energy Chem. 65 (2022) 280–292.
[97] W. Qiu, X.L. Huang, Y. Wang, C. Feng, H. Ji, H.K. Liu, S.X. Dou, Z. Wang, J. Energy Chem. 76 (2023) 528–546.
[98] P. Guan, L. Zhou, Z. Yu, Y. Sun, Y. Liu, F. Wu, Y. Jiang, D. Chu, J. Energy Chem. 43 (2020) 220–235.
[99] C. Hakim, N. Sabi, I. Saadoune, J. Energy Chem. 61 (2021) 47–60.
[100] S. Zhao, Z. Liu, G. Xie, Z. Guo, S. Wang, J. Zhou, X. Xie, B. Sun, S. Guo, G. Wang, Energy Environ. Sci. 15 (2022) 3015–3023.
[101] B. Larhrib, L. Madec, L. Monconduit, H. Martinez, J. Power Sources 588 (2023) 233743.
[102] L. Liang, M. Tang, Q. Zhu, W. Wei, S. Wang, J. Wang, J. Chen, D. Yu, H. Wang, Adv. Energy Mater. 13 (2023) 2300453.
[103] L.H.B. Nguyen, P.S. Camacho, J. Fondard, D. Carlier, L. Croguennec, M.R. Palacin, A. Ponrouch, C. Courrèges, R. Dedryvère, K. Trad, C. Jordy, S. Genies, Y. Reynier, L. Simonin, J. Power Sources 529 (2022) 231253.
[104] Y.-S. Duh, Y. Sun, X. Lin, J. Zheng, M. Wang, Y. Wang, X. Lin, X. Jiang, Z. Zheng, S. Zheng, G. Yu, J. Energy Storage 41 (2021) 102888.
[105] C. Shen, K. Yuan, T. Tian, M. Bai, J.-G. Wang, X. Li, K. Xie, Q.-G. Fu, B. Wei, ACS Appl. Mater. Interfaces 11 (2019) 5015–5021.
[106] W.-C. Chang, J.-H. Wu, K.-T. Chen, H.-Y. Tuan, Adv. Sci. 6 (2019) 1801354.
[107] Q. Sun, D. Li, J. Cheng, L. Dai, J. Guo, Z. Liang, L. Ci, Carbon 155 (2019) 601–610.
[108] J.-Z. Guo, Z.-Y. Gu, X.-X. Zhao, M.-Y. Wang, X. Yang, Y. Yang, W.-H. Li, X.-L. Wu, Adv. Energy Mater. 9 (2019) 1902056.
[109] S.-B. Huang, Y.-Y. Hsieh, K.-T. Chen, H.-Y. Tuan, Chem. Eng. J. 416 (2021) 127697.

[110] C.-Y. Tsai, C.-H. Chang, T.-L. Kao, K.-T. Chen, H.-Y. Tuan, Chem. Eng. J. 417 (2021) 128552.
[111] Z. Luo, D. Chen, X. Wang, J. Huang, Y. Pan, W. Lei, J. Pan, Small 17 (2021) 2008163.
[112] F. Qiao, J. Meng, J. Wang, P. Wu, D. Xu, Q. An, X. Wang, L. Mai, J. Mater. Chem. A. 9 (2021) 23046–23054.
[113] B. Han, D. Zhang, X. Liu, Z. Wang, W. Qu, S. Zhang, C. Deng, J. Mater. Chem. A. 10 (2022) 13508–13518.
[114] T. Wang, Q. Liu, J. Zhou, X. Wang, B. Lu, Adv. Energy Mater. 12 (2022) 2202357.
[115] S.-L. Chou, Y. Pan, J.-Z. Wang, H.-K. Liu, S.-X. Dou, Phys. Chem. Chem. Phys. 16 (2014) 20347–20359.
[116] A. Kraytsberg, Y. Ein-Eli, Adv. Energy Mater. 6 (2016) 1600655.
[117] W. Zhang, M. Dahbi, S. Komaba, Curr. Opin. Chem. Eng. 13 (2016) 36–44.
[118] M.Á. Muñoz-Márquez, M. Zarrabeitia, S. Passerini, T. Rojo, Adv. Mater. Interfaces 9 (2022) 2101773.
[119] Y. He, L. Jing, Y. Ji, Z. Zhu, L. Feng, X. Fu, Y. Wang, J. Energy Chem. 72 (2022) 41–55.
[120] Y. Zhang, Y. Zhu, S. Zheng, L. Zhang, X. Shi, J. He, X. Chou, Z.-S. Wu, J. Energy Chem. 63 (2021) 498–513.
[121] M. Liu, L. Chang, Z. Le, J. Jiang, J. Li, H. Wang, C. Zhao, T. Xu, P. Nie, L. Wang, ChemSusChem. 13 (2020) 5837–5862.
[122] S.M. Ahmed, G. Suo, W.A. Wang, K. Xi, S.B. Iqbal, J. Energy Chem. 62 (2021) 307–337.
[123] W. Zhao, X. Shi, B. Liu, H. Ueno, T. Deng, W. Zheng, J. Energy Chem. 89 (2023) 579–598.